Inorganic Chemistry

ARTICLE

pubs.acs.org/IC

Synthesis and Structure of Dawson Polyoxometalate-Based, Multifunctional, Inorganic−Organic Hybrid Compounds: Organogermyl Complexes with One Terminal Functional Group and Organosilyl Analogues with Two Terminal Functional Groups

Kenji Nomiya,* Yoshihiro Togashi, Yuhki Kasahara, Shotaro Aoki, Hideaki Seki, Marie Noguchi, and Shoko Yoshida

Department of Chemistry (formerly Department of Materials Science), Faculty of Science, Kanagawa University, Hiratsuka, Kanagawa 259-1293, Japan

Supporting Information

ABSTRACT:

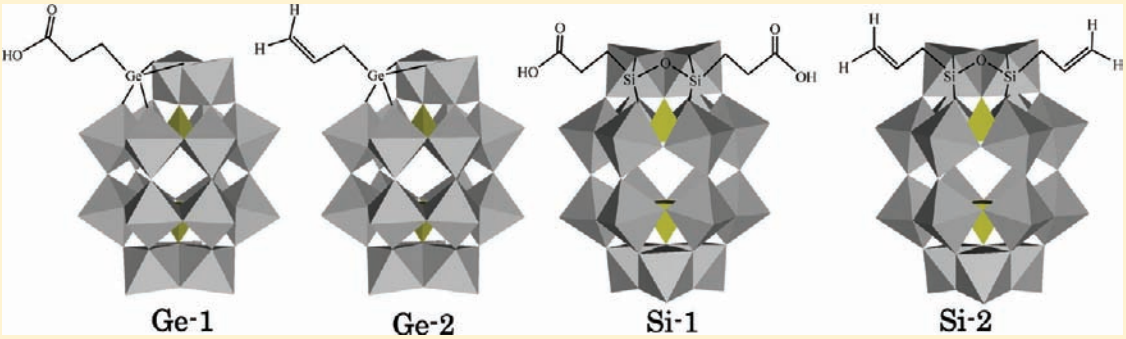

Four novel multifunctional polyoxometalate (POM)-based inorganic−organic hybrid compounds, $[\alpha_2\text{-}P_2W_{17}O_{61}\{(RGe)\}]^{7-}$ (**Ge-1**, R_1 = $HOOC(CH_2)_2$- and **Ge-2**, R_2 = $H_2C{=}CHCH_2$-) and $[\alpha_2\text{-}P_2W_{17}O_{61}\{(RSi)_2O\}]^{6-}$ (**Si-1**, R_1 and **Si-2**, R_2), were prepared by incorporating organic chains having terminal functional groups (carboxylic acid and allyl groups) into monolacunary site of Dawson polyoxoanion $[\alpha_2\text{-}P_2W_{17}O_{61}]^{10-}$. In these POMs, new modification of the terminal functional groups was attained by introducing organogermyl and organosilyl groups. Dimethylammonium salts of the organogermyl complexes, $(Me_2NH_2)_7[\alpha_2\text{-}P_2W_{17}O_{61}(R_1Ge)]\cdot H_2O$ **MeN-Ge-1** and $(Me_2NH_2)_7[\alpha_2\text{-}P_2W_{17}O_{61}(R_2Ge)]\cdot 4H_2O$ **MeN-Ge-2**, were obtained as analytically pure crystals, in 22.8% and 55.3% yields, respectively, by stoichiometric reactions of $[\alpha_2\text{-}P_2W_{17}O_{61}]^{10-}$ with separately prepared $Cl_3GeC_2H_4COOH$ in water, and $H_2C{=}CHCH_2GeCl_3$ in a solvent mixture of water/acetonitrile. Synthesis and X-ray structure analysis of the Dawson POM-based organogermyl complexes were first successful. Dimethylammonium salts of the corresponding organosilyl complexes, $(Me_2NH_2)_6[\alpha_2\text{-}P_2W_{17}O_{61}\{(R_1Si)_2O\}]\cdot 4H_2O$ **MeN-Si-1** and $(Me_2NH_2)_6[\alpha_2\text{-}P_2W_{17}O_{61}\{(R_2Si)_2O\}]\cdot 6H_2O$ **MeN-Si-2**, were also obtained as analytically pure crystalline crystals, in 17.1% and 63.5% yields, respectively, by stoichiometric reactions of $[\alpha_2\text{-}P_2W_{17}O_{61}]^{10-}$ with $NaOOC(CH_2)_2Si(OH)_2(ONa)$ and $H_2C{=}CHCH_2Si(OEt)_3$. These complexes were characterized by elemental analysis, thermogravimetric and differential thermal analyses (TG/DTA), FTIR, solid-state (^{31}P) and solution (^{31}P, ^{1}H, and ^{13}C) NMR, and X-ray crystallography.

INTRODUCTION

Polyoxometalates (POMs) are discrete metal oxide clusters that are of current interest as soluble metal oxides and for their applications in catalysis, medicine, and materials science.[1] The preparation of POM-based materials is therefore an active field of research and, in particular, the combination of POMs with organic molecules has brought about a variety of inorganic−organic hybrid materials.[2−8] The introduction of organic groups into POMs is an efficient technology to significantly increase the number of inorganic−organic hybrid compounds and to improve their properties. The POM-based inorganic−organic hybrid compounds are classified as organostanyl, organophosphoryl, organo-transition metal, organosilyl and organogermyl complexes, and so on.[2−8] Although many examples of X-ray structure analysis of the complexes have been reported,[3−7] those of the organogermyl complexes have scarcely been reported.[8] The inorganic−organic hybrid compounds are also classified based on the Keggin POM-family,[3−5] Dawson POM-family,[6] and others.[7]

Various types of Keggin POM-based inorganic−organic hybrid compounds have been determined by X-ray crystallography.[3−5]

Received: June 22, 2011
Published: September 08, 2011

These include, for example, monolacunary Keggin POM-based compounds such as $[PW_{11}O_{39}(PhPO)_2]^{3-}$,[3a] $[PW_{11}O_{39}\{Rh_2(OAc)_2\}]^{5-}$,[3b] $[\alpha\text{-}PW_{11}O_{39}\{(HS(CH_2)_3Si)_2O\}]^{3-}$,[5p] dilacunary Keggin POM-based compounds such as $[(\gamma\text{-}SiW_{10}O_{36})_2\{PhSn(H_2O)\}_2]^{10-}$,[4a] $[\gamma\text{-}PW_{10}O_{36}(^tBuSiOH)_2]^{3-}$,[4c] and trilacunary Keggin POM-based compounds such as $[(PW_9O_{34})_2(PhSnOH)_3]^{12-}$,[5a] $[\beta\text{-}SiW_9O_{37}(PhSn)_3]^{7-}$,[5b] $[(\alpha\text{-}SiW_9O_{34})_2(BuSnOH)_3]^{14-}$,[5b] $[A\text{-}\alpha\text{-}PW_9O_{34}(^tBuSiOH)_3]^{3-}$,[5c] and $[B\text{-}\alpha\text{-}AsW_9O_{33}(^tBuSiOH)_3]^{3-}$,[5c] $[A\text{-}\alpha\text{-}PW_9O_{34}\{(RSiO)_3(RSi)\}]^{3-}$ (R = C_2H_3, CH_3, C_2H_5),[5e,f] $[A\text{-}\alpha\text{-}PW_9O_{34}\{(^tBuSiO)_3(SiCH_2CH{=}CH_2)\}]^{3-}$,[5g] $[A\text{-}PW_9O_{34}\{(HS(CH_2)_3SiOH)_3\}]^{3-}$,[5p] and $[A\text{-}\alpha\text{-}PW_9O_{34}\{(HS(CH_2)_3SiO)_3(Si(CH_2)_3SH)\}]^{3-}$.[5p]

The molecular structures of Dawson POM-based inorganic−organic hybrid compounds have also been determined, such as $[\alpha\text{-}P_2W_{15}O_{59}(PhSn)_3]^{9-}$,[5a] $[\alpha_2\text{-}P_2W_{17}O_{61}\{(C_6H_6)Ru(H_2O)\}]^{8-}$,[6a] and $[\alpha_2\text{-}P_2W_{17}O_{61}\{(RSi)_2O\}]^{6-}$ (organic groups with terminal functional groups: R = Ph, $HS(CH_2)_3-$, $NCS(CH_2)_3-$,[6b] and $Me_3N^+(CH_2)_3-$,[6c] and organic groups with terminal olefins: R = $\{H_2C{=}C(CH_3)OCO(CH_2)_3-\}$, $\{H_2C{=}CHOCO(CH_2)_3-\}$ and $\{H_2C{=}CH-\}$).[6d] X-ray crystallography has revealed that organosilyl groups have been grafted as two organic chains connected by a siloxane bond (Si−O−Si bond) onto an α_2-monolacunary site of a Dawson POM (POM: organic group = 1:2 complex).

Many other inorganic−organic hybrid compounds, characterized by X-ray crystallography, can also be found in recent literature.[7]

As for the organogermyl complexes, we know of only a few examples of X-ray structure analysis reported so far; Keggin POM-based organosilyl/-germyl hybrids, such as $[PW_9O_{34}\{(^tBuSiO)_3Ge(CH_2)_2CO_2H\}]^{3-}$,[8b] and a Dawson POM-based organogermyl compound, $[\alpha_2\text{-}P_2W_{17}O_{61}(GeOH)]^{7-}$, although the Ge site in the latter was not determined due to disorder of an α-Dawson structure.[6e] In contrast to 1:2 complexes consisting of organosilyl groups, organogermyl groups grafted onto POMs have been known as Keggin POM: organic group = a 1:1 complex such as $[TW_{11}O_{39}(GeCH_2CH_2X)]^{n-}$ (T = Si, Ge, Ga; X = −COOH, $-COOCH_3$, $-CONH_2$, −CN; n = 5, 6),[8a] but their X-ray structure analyses have not been reported.

From a practical point of view, the heterogenization or immobilization of POM-based acid and oxidation catalysts is expedient owing to the ease of recycling and separation of these catalysts from the reaction products. Some of the modified POMs with organic functional groups, such as thiol, vinyl, and methacryl groups, can be used as precursors for the immobilization of POMs.[2i,o,p,8a] For example, for fuel-cell applications, the preparation and characterization of a proton-conducting membrane using $[SiW_{11}O_{39}\{(CH_2{=}CHSi)_2O\}]^{4-}$ has been reported.[9a] In the platinum electrode of a fuel cell, which was modified with a Dawson-type inorganic−organic hybrid POM with a terminal −SH group, the catalytic activity was found to be enhanced.[9b]

In this work, to extend the chemistry of POM-based inorganic−organic hybrid compounds containing multifunctional groups, we examined the reactions of a monolacunary Dawson POM, $[\alpha_2\text{-}P_2W_{17}O_{61}]^{10-}$ with separately prepared 3-(trichlorogermyl)propionic acid ($Cl_3GeC_2H_4COOH$) in water and allyltrichlorogermane ($H_2C{=}CHCH_2GeCl_3$) in a sovent mixture of water/acetonitrile, respectively. We also examined the reactions of $[\alpha_2\text{-}P_2W_{17}O_{61}]^{10-}$ with the sodium salt of carboxyethylsilane triol ($NaOOC(CH_2)_2Si(OH)_2(ONa)$) and allyltriethoxysilane ($H_2CCHCH_2Si(OEt)_3$), respectively. Herein, we successfully obtained a series of Dawson-type POM-based, organogermyl and organosilyl complexes including organic chains having terminal −COOH and allyl groups, which have not been reported so far, that is, two organogermyl complexes, $(Me_2NH_2)_7[\alpha_2\text{-}P_2W_{17}O_{61}(R_1Ge)]\cdot H_2O$ **MeN-Ge-1** and $(Me_2NH_2)_7[\alpha_2\text{-}P_2W_{17}O_{61}(R_2Ge)]\cdot 4H_2O$ **MeN-Ge-2** (R_1 = $HOOC(CH_2)_2-$ and R_2 = $H_2C{=}CHCH_2-$) and two organosilyl complexes, $(Me_2NH_2)_6[\alpha_2\text{-}P_2W_{17}O_{61}\{(R_1Si)_2O\}]\cdot 4H_2O$ **MeN-Si-1** and $(Me_2NH_2)_6[\alpha_2\text{-}P_2W_{17}O_{61}\{(R_2Si)_2O\}]\cdot 6H_2O$ **MeN-Si-2**. [Note: the moieties of the polyoxoanions were simply abbreviated as $[\alpha_2\text{-}P_2W_{17}O_{61}(RGe)]^{7-}$ (**Ge-1**, R_1 and **Ge-2**, R_2) and $[\alpha_2\text{-}P_2W_{17}O_{61}\{(RSi)_2O\}]^{6-}$ (**Si-1**, R_1 and **Si-2**, R_2).

In this paper, we report full details of the synthesis and unequivocal characterization of these four complexes and their molecular structures.

EXPERIMENTAL SECTION

Materials. The following reagents were used as received: EtOH, MeOH, CH_3CN, Et_2O, *n*-hexane, Me_2NH_2Cl, 12, 6, and 1 M aqueous HCl solutions, 85% phosphoric acid, acrylic acid, GeO_2 (all from Wako); allyltrichlorogermane ($H_2C{=}CHCH_2GeCl_3$), allyltriethoxysilane ($H_2C{=}CHCH_2Si(OEt)_3$), sodium salt of carboxyethylsilane triol, (25% in water) ($NaOOC(CH_2)_2Si(OH)_2ONa$) (all from Gelest); D_2O, DCl (35 wt% in D_2O) CD_3CN, DMSO-d_6 (all from Isotec). Monolacunary Dawson POMs, $K_{10}[\alpha_2\text{-}P_2W_{17}O_{61}]\cdot xH_2O$ (x = 15, 23, 24)*, were prepared according to the literature[12] and identified by FTIR, TG/DTA, and ^{31}P NMR.

*Different hydrated species of $K_{10}[\alpha_2\text{-}P_2W_{17}O_{61}]\cdot xH_2O$ were used for the syntheses of the POMs: the compounds with x = 24 and 15 were used for the **MeN-Ge-1** and **MeN-Si-1** syntheses, respectively. The compound with x = 23 was used for the **MeN-Ge-2** and **MeN-Si-2** syntheses.

Instrumentation/Analytical Procedures. Elemental analyses were carried out with a Perkin−Elmer 2400 CHNS Elemental Analyzer II (Kanagawa University). Infrared spectra were recorded on a Jasco 4100 FT-IR spectrometer in KBr disks at room temperature. Thermogravimetric (TG) and differential thermal analyses (DTA) were acquired using a Rigaku Thermo Plus 2 series TG/DTA TG 8120 instrument. TG/DTA measurements were run under air with a temperature ramp of 4 °C per min between 20 and 500 °C.

^1H (399.65 MHz), $^{13}C\{^1H\}$ (100.40 MHz), and ^{31}P (161.70 MHz) spectra in water (D_2O, or 6 M HCl aq., or 6 M DCl aq.) and CD_3CN were recorded in 5 mm outer diameter tubes on a JEOL JNM-EX 400 FT-NMR spectrometer and a JEOL EX-400 NMR data-processing system. ^1H (500.16 MHz), $^{13}C\{^1H\}$ (125.78 MHz), and ^{31}P (202.47 MHz) NMR spectra in water (D_2O, or 6 M HCl aq., or 6 M DCl aq.) and CD_3CN were recorded in 5 mm outer diameter tubes on a JEOL ECP 500 FT-NMR spectrometer using a JEOL ECP-500 NMR data-processing system. ^1H and $^{13}C\{^1H\}$NMR spectra were measured in water (D_2O, or 6 M HCl aq., or 6 M DCl aq.) and CD_3CN with references to internal DSS or tetramethylsilane ($SiMe_4$). ^{31}P NMR spectra were referenced to an external standard of 25% H_3PO_4 in H_2O in a sealed capillary. The ^{31}P NMR data with the usual 85% H_3PO_4 reference are shifted to +0.544 ppm from our data. Solid-state ^{31}P (121.00 MHz) CPMAS NMR spectra were recorded in 6 mm outer diameter rotors on a JEOL JNM-ECP 300 FT-NMR spectrometer with a JEOL ECP-300 NMR data-processing system. These spectra were referenced to an external standard, $(NH_4)_2HPO_4$, and polydimethylsilane. Chemical shifts are reported as negative for resonances upfield of $(NH_4)_2HPO_4$ (δ 1.60).

Preparation of $Cl_3Ge(CH_2)_2COOH$. To a suspension of GeO_2 (10.46 g, 0.10 mol) in approximately 120 mL of a 12 M aqueous HCl solution was added 50% phosphinic acid (H_3PO_2 d 1.20−1.23; 16 mL,

approximately 0.15 mol). The white suspension was stirred for 3 h in a water bath at 90 °C. After cooling to room temperature, acrylic acid (H_2C═CHCOOH d 1.050−1.060; 7.2 g, 0.10 mol) cooled in an ice-bath was slowly added using a pipet. [Note: The temperature of the solution increased by adding acrylic acid. On increasing the temperature, acrylic acid readily polymerizes.] The solution was stirred for 1 h at room temperature and further for 30 min in an ice-bath. The white powder that formed was collected on a membrane filter (JG 0.2 μm). The powder was dissolved in 150 mL of *n*-hexane in a water bath at 70 °C. The solution formed two layers. The lower layer in the water bath at 70 °C was removed using a pipet. After the upper layer was cooled to room temperature, the solution was placed overnight in a refrigerator at approximately 4 °C. The white crystals that formed were collected on a membrane filter (JG 0.2 μm), washed with *n*-hexane (50 mL, 3 times), and dried in vacuo for 2 h. The white powder, obtained in 72.8% (18.34 g scale) yield, was very soluble in most organic solvents, such as MeOH, EtOH, acetone, CH_3CN, EtOAc, chloroform, and dichloromethane, and soluble in water, but sparingly soluble in hexane. Found: C, 14.33%; H, 1.81%. Calcd. for $Cl_3Ge_3C_2H_4$-COOH: C, 14.30%; H, 2.00%. TG/DTA under atmospheric conditions: a weight loss of 71.47% was observed below 500 °C with the melting point at 86.1 °C and endothermic points at 297.5−319.6 °C. ^{1}H NMR (22.3 °C, CD_3CN): δ 2.39 (2H, t, H1), 2.83 (2H, t, H2), 9.56 (COOH). ^{13}C NMR (23.8 °C, CD_3CN): δ 28.39 (C1), 29.70 (C2), 175.45 (COOH).

Preparation of $(Me_2NH_2)_7[\alpha_2$-$P_2W_{17}O_{61}(HOOC(CH_2)_2Ge)]\cdot H_2O$ (MeN-Ge-1). To a colorless clear aqueous solution of Cl_3Ge-$(CH_2)_2COOH$ (0.25 g, 1.0 mmol) dissolved in 30 mL of water was added solid $K_{10}[\alpha_2$-$P_2W_{17}O_{61}]\cdot 24H_2O$ (5.0 g, 1.0 mmol). After stirring for 30 min, Me_2NH_2Cl (5.5 g, 67.5 mmol) was added. The white powder that formed was collected on a membrane filter (JG 0.2 μm), washed with EtOH (30 mL, 3 times) and Et_2O (50 mL, 3 times), and dried in vacuo for 2 h. The white powder, obtained in 88.8% (4.16 g scale) yield, was soluble in water and DMSO but insoluble in CH_3CN.

Crystallization. The powder (1.5 g) was dissolved in 4 mL of water in a water bath at 80 °C. After cooling to room temperature, slow evaporation was performed in a dark at room temperature. After 1 day, the colorless plate crystals that formed were collected on a membrane filter (JG 0.2 μm), washed with EtOH (30 mL, 3 times) and Et_2O (50 mL, 3 times), and dried in vacuo for 2 h. Yield: 22.8% (0.34 g scale). Found: C, 4.32%; H, 1.24%; N, 2.06%. Calcd. for $(Me_2NH_2)_7[\alpha_2$-$P_2W_{17}O_{61}\{HOOC$-$(CH_2)_2Ge\}]\cdot H_2O$ or $C_{17}H_{63}N_7O_{70}GeP_2W_{17}$: C, 4.39%; H, 1.37%; N, 2.11%. TG/DTA under atmospheric conditions: a weight loss of 0.51% was observed below 153.4 °C with an endothermic point at 94.8 °C based on dehydration; calcd. 0.39% for x = 1 in $(Me_2NH_2)_7[P_2W_{17}O_{61}$-$\{HOOC(CH_2)_2Ge\}]\cdot xH_2O$ and a weight loss of 6.96% was observed between 153.4 and 501.3 °C with an endothermic point at 205.8 °C and exothermic points at 298.2 and 384.9 °C based on decomposition of the countercation and the terminal −COOH group. FTIR (KBr): 1705 m [−COOH], 1612 s, 1504 w, 1464 s, 1439 w, 1414 w, 1375 w, 1230 m, 1086 vs, 1016 m, 953 vs, 924 w, 899 w, 771 vs, 665 w, 613 w, 600 w, 565 w, 525 m, 486 w, 469 w, 434 w cm^{-1}. Solid-state CPMAS ^{31}P NMR: δ −9.5, −12.9. ^{31}P NMR (23.5 °C, D_2O): δ −10.27, −13.57. ^{1}H NMR (21.3 °C, D_2O): δ 1.45 (1H, t, H1), 2.77(22H, s, Me_2NH_2 + H2). ^{13}C NMR (22.4 °C, D_2O): δ 22.57 (C1), 30.90 (C2), 180.99(CO_2H), 37.10 (Me_2NH_2).

Preparation of $(Me_2NH_2)_7[\alpha_2$-$P_2W_{17}O_{61}(H_2C$═$CHCH_2Ge)]\cdot 4H_2O$ (MeN-Ge-2). To a solution of allyltrichlorogermane (H_2C═$CHCH_2GeCl_3$ 144 μL, 1.0 mmol) dissolved in 60 mL of acetonitrile was added 50 mL of water and solid $K_{10}[\alpha_2$-$P_2W_{17}O_{61}]\cdot 23H_2O$ (5.0 g, 1.0 mmol). To that 5 mL of a 1 M aqueous HCl solution was added. After stirring for 1 h at room temperature, the resulting pale yellow solution was concentrated to approximately 50 mL of volume with a rotary evaporator at 30 °C. To it was added Me_2NH_2Cl (5.5 g, 67.5 mmol). After stirring for 1 h in an ice bath, the pale-yellow powder that formed was collected on a membrane filter (JG 0.2 μm), washed with EtOH (30 mL, 2 times) and Et_2O (50 mL, 2 times), and dried in vacuo for 2 h in the dark. At this stage, a pale-yellow powder was obtained in a yield of 4.59 g.

Crystallization. The pale-yellow powder (1.35 g) was dissolved in 4 mL of water. The solution was slowly evaporated at room temperature in the dark. After 7 h, the yellow rod crystals that formed were collected on a membrane filter (JG 0.2 μm), washed with EtOH (30 mL, 2 times) and Et_2O (50 mL, 2 times), and dried in vacuo for 2 h in the dark, and obtained in 55.3% yield (0.83 g scale). The crystals obtained were soluble in water, dimethyl sulfoxide, sparingly soluble in acetone, but insoluble in methanol, ethanol, acetonitrile, chloroform, dichloromethane, and diethyl ether. Found: C, 4.37%; H, 1.49%; N, 2.10%. Calcd. for $(Me_2NH_2)_7[\alpha_2$-$P_2W_{17}O_{61}(H_2CCHCH_2Ge)]\cdot 4H_2O$ or $C_{17}H_{69}N_7O_{65}Ge_1P_2W_{17}$: C, 4.40%; H; 1.12%; N; 2.23%. TG/DTA under atmospheric conditions: a weight loss of 1.62% was observed below at 142.9 °C based on dehydration; calcd. 1.54% for x = 4 in $(Me_2NH_2)_7[\alpha_2$-$P_2W_{17}O_{61}(H_2C$═$CHCH_2Ge)]\cdot xH_2O$ and a weight loss of 6.87% was observed between 142.9 and 501.4 °C with exothermic points at 360.6 and 415.6 °C based on decomposition of the $Me_2NH_2^+$ cation and allyl group. FTIR (KBr): 1615 m, 1464 s, 1415 w, 1087 vs, 1018 m, 953 vs, 920 vs, 769 vs, 599 s, 565 m, 523 s, 485 m, 469 m, 431 m cm^{-1}. Solid-state CPMAS ^{31}P NMR: δ −9.6, −12.7. ^{31}P NMR (22.8 °C, D_2O): δ −10.20, −13.53. ^{1}H NMR (23.5 °C, D_2O): δ 2.15−2.17 (2H, d, H1), 5.01−5.04 (1H, d, H3a, J = 10.0 Hz), 5.11−5.15 (1H, d, H3b, J = 17.1 Hz), 5.99−6.10 (1H, sext, H2), 2.80 (Me_2NH_2). [Note: H3a and H3b are designated as in *cis*- and *trans*-positions in regard to H2, respectively.] ^{13}C NMR (24.2 °C, D_2O): δ 34.24 (C1), 118.8 (C3), 135.3 (C2), 37.53 (Me_2NH_2).

Preparation of $(Me_2NH_2)_6[\alpha_2$-$P_2W_{17}O_{61}\{(HOOC(CH_2)_2Si)_2$-$O\}]\cdot 4H_2O$ (MeN-Si-1). A silane-coupling agent, sodium salt of carboxyethylsilane triol ($NaOOC(CH_2)_2Si(OH)_2(ONa)$, 25% in water, d 1.17; 1.34 mL, 2.0 mmol) was added to 80 mL of water. To it was added solid $K_{10}[\alpha_2$-$P_2W_{17}O_{61}]\cdot 15H_2O$ (4.9 g, 1.0 mmol). The pH of the dispersion was adjusted to <0.5 using 6 and 1 M aqueous HCl solutions. The color of the solution gradually changed to pale yellow and was evaporated to approximately 20 mL of volume using a rotary evaporator at 35 °C. To it was added Me_2NH_2Cl (5.5 g, 67.5 mmol). The white precipitate that formed was collected on a membrane filter (JG 0.2 μm), washed with ethanol (30 mL, 3 times) and Et_2O (50 mL, 3 times), and then dried in vacuo for 2 h. The powder sample, obtained in 80.7% (3.86 g scale) yield, was soluble in water and DMSO but insoluble in acetonitrile, acetone, MeOH, EtOH, EtOAc, dichloromethane, and Et_2O. This compound was stable in the solid state and only in a 6 M HCl solution, but it readily decomposed in water. In a 1 M HCl solution, it slowly decomposed.

Crystallization. The white powder (1.0 g) was dissolved in 4 mL of a 1 M aqueous HCl solution. The solution was passed through a folded filter paper (Whatman #2). The filtrate was slowly evaporated at room temperature in the dark. After 4 days, pale yellow rod crystals formed, which were collected on a membrane filter (JG 0.2 μm), washed with Et_2O (50 mL, 3 times), and then dried in vacuo for 2 h. Yield: 17.1% (0.18 g scale). Found: C, 4.65%; H, 1.26%; N, 1.84%. Calcd. for $(Me_2NH_2)_6[\alpha_2$-$P_2W_{17}O_{61}\{HOOC(CH_2)_2Si\}_2O]\cdot 4H_2O$ or $C_{18}H_{66}N_6O_{70}Si_2P_2W_{17}$: C, 4.57%; H, 1.41%; N, 1.78%. TG/DTA under atmospheric conditions: a weight loss of 1.43% was observed below 229.7 °C with an endothermic point at 54.0 °C based on dehydration; calcd. 1.52% for x = 4 in $(Me_2NH_2)_6[P_2W_{17}O_{61}\{HOOC(CH_2)_2Si\}_2O]\cdot xH_2O$ and a weight loss of 8.19% was observed between 229.7 and 502.1 °C with an endothermic point at 391.1 °C based on decomposition of the $Me_2NH_2^+$ cation and the terminal −COOH groups. FTIR (KBr): 1728 m [COOH], 1607 m, 1466 s, 1439 w, 1416 m, 1284 w, 1222 w, 1088 vs, 1041 vs, 957 vs, 925 vs, 797 vs, 607 w, 597 w, 566 m, 529 m, 485 m cm^{-1}. Solid-state CPMAS ^{31}P NMR: δ −9.5, −12.7. ^{31}P NMR (23.3 °C, D_2O): δ −10.25, −13.25 (major peaks); −8.45, −13.10 (minor peaks due to the monolacunary Dawson POM). ^{31}P NMR (23.2 °C, 6 M HCl aq.): δ −10.37, −13.42. ^{1}H NMR (23.1 °C,

6 M DCl aq.): δ 1.11 (1H, t, H1), 2.70 (1H, d, H2), 2.78 (Me_2NH_2). ^{13}C NMR (25.4 °C, 6 M HCl aq.): δ 8.91 (C1), 29.58 (C2), 181.1 (CO_2H), 37.56 (Me_2NH_2).

Preparation of $(Me_2NH_2)_6[\alpha_2\text{-}P_2W_{17}O_{61}\{(H_2C{=}CHCH_2Si)_2O\}]\cdot 6H_2O$ (MeN-Si-2). To a solution of allyltriethoxysilane ($H_2C{=}CHCH_2Si(OEt)_3$ 453 μL, 2.0 mmol) dissolved in 60 mL of acetonitrile were added 100 mL of water and solid $K_{10}[\alpha_2\text{-}P_2W_{17}O_{61}]\cdot 23H_2O$ (5.0 g, 1.0 mmol). The pH of the dispersion was adjusted to 1.5 with a 1 M aqueous HCl solution. After stirring for 30 min at room temperature, the resulting yellow solution was concentrated to approximately 20 mL of volume with a rotary evaporator at 30 °C. To it was added Me_2NH_2Cl (5.5 g, 67.5 mmol). After stirring for 1 h in an ice bath, the yellow powder that formed was collected on a membrane filter (JG 0.2 μm), washed with MeOH (30 mL, 2 times) and Et_2O (50 mL, 2 times), and dried in vacuo for 2 h in the dark. At this stage, yellow powder was obtained in a yield of 3.58 g.

Crystallization. The pH of a solution of yellow powder (1.0 g) dissolved in 5 mL of water was adjusted to 2.0 with a 1 M aqueous HCl solution. The solution was slowly evaporated at room temperature in the dark. After 3 days, the yellow rod crystals that formed were collected on a membrane filter (JG 0.2 μm), washed with MeOH (30 mL, 2 times) and Et_2O (50 mL, 2 times), and dried in vacuo for 2 h in the dark, and obtained in 63.5% yield (0.63 g scale). The crystals obtained were soluble in water and dimethyl sulfoxide, but insoluble in methanol, ethanol, acetonitrile, acetone, chloroform, dichloromethane, and diethyl ether. Found: C, 4.71%; H, 1.36%; N, 1.73%. Calcd. for $(Me_2NH_2)_6[\alpha_2\text{-}P_2W_{17}O_{61}\{(H_2C{=}CHCH_2Si)_2O\}]\cdot 6H_2O$ or $C_{18}H_{70}N_6O_{68}Si_2P_2W_{17}$: C, 4.60%; H;1.50%; N;1.79%. TG/DTA under atmospheric conditions: a weight loss of 2.12% was observed at below 119.3 °C based on dehydration; calcd. 2.30% for $x = 6$ in $(Me_2NH_2)_6[\alpha_2\text{-}P_2W_{17}O_{61}\{(H_2CCHCH_2Si)_2O\}]\cdot xH_2O$ and a weight loss of 6.05% was observed between 119.3 and 501.2 °C with exothermic points at 242.0 and 393.8 °C based on decomposition of the $Me_2NH_2^+$ cation and allyl groups. FTIR (KBr): 1618 m, 1466 m, 1417 m, 1173 m, 1089 s, 1041 s, 955 vs, 921 s, 796 vs, 565 m, 529 m, 479 w, 415 w cm^{-1}. Solid-state CPMAS ^{31}P NMR: δ −9.9, −13.1. ^{31}P NMR (22.1 °C, D_2O): δ −10.28, −13.30 (major peaks); −8.31, −13.36 (minor peaks due to the monolacunary Dawson POM). ^{31}P NMR (22.3 °C, 6 M HCl aq., just after dissolving): δ −10.40, −13.41. ^1H NMR (23.1 °C, D_2O, just after dissolving): δ 1.83−1.85 (2H, d, H1), 5.06−5.08 (1H, d, H3a, J = 10.0 Hz), 5.15−5.19 (1H, d, H3b, J = 17.4 Hz), 5.94−6.03 (1H, sext, H2), 2.79 (Me_2NH_2). ^{13}C NMR (25.5 °C, D_2O, just after dissolving): δ 21.57 (C1), 118.7 (C3), 134.5 (C2), 37.47 (Me_2NH_2).

X-ray Crystallography. Crystals of compounds **MeN-Ge-1**, **MeN-Ge-2**, **MeN-Si-1**, and **MeN-Si-2** were covered with Paratone-N (liquid paraffin) to prevent their degradation. The crystal sizes were 0.12 × 0.08 × 0.05 mm^3 (**MeN-Ge-1**), 0.30 × 0.11 × 0.02 mm^3 (**MeN-Ge-2**), 0.26 × 0.09 × 0.05 mm^3 (**MeN-Si-1**), and 0.30 × 0.08 × 0.02 mm^3 (**MeN-Si-2**). Data collection was done with a Bruker SMART APEX CCD diffractometer at 90 K in the range of $0.82° < \theta < 28.53°$ (**MeN-Ge-1**), $1.55° < \theta < 28.31°$ (**MeN-Ge-2**), $1.00° < \theta < 28.34°$ (**MeN-Si-1**), and $0.84° < \theta < 23.28°$ (**MeN-Ge-1**). The intensity data were automatically corrected for Lorentz and polarization effects during integration. The structure was obtained by direct methods (*SHELXS-97*),[13a] followed by a difference Fourier calculation, and refined by a full-matrix, least-squares procedure on F^2 (program *SHELXL-97*).[13b] Absorption correction was performed with *SADABS* (empirical absorption correction).[13c] The composition and formula of the POM containing many counterions and several hydrated water molecules were determined by elemental analysis and TG/DTA analysis. Refinements of the positions and temperature factors of many counterions and several solvent molecules in the POM are limited because of their disorder. We can reveal only the molecular structure of the POM but not the crystal structure. These features are very common in POM crystallography.

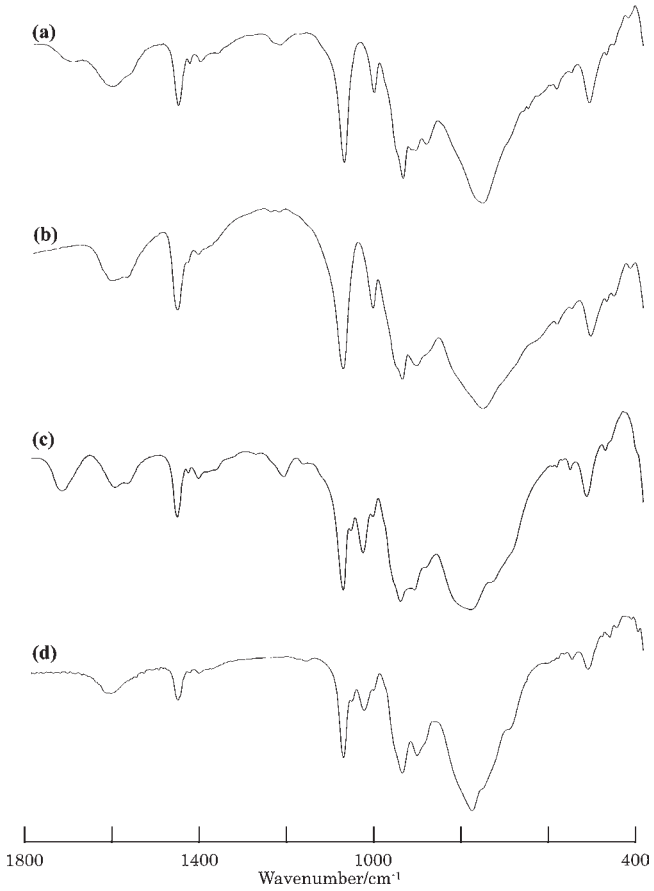

Figure 1. FTIR spectra in the polyoxoanion region (1800−400 cm^{-1}), measured as KBr disks, of (a) $(Me_2NH_2)_7[\alpha_2\text{-}P_2W_{17}O_{61}(HOOC(CH_2)_2Ge)]\cdot H_2O$ **MeN-Ge-1**, (b) $(Me_2NH_2)_7[\alpha_2\text{-}P_2W_{17}O_{61}(H_2C{=}CHCH_2Ge)]\cdot 4H_2O$ **MeN-Ge-2**, (c) $(Me_2NH_2)_6[\alpha_2\text{-}P_2W_{17}O_{61}\{(HOOC(CH_2)_2Si)_2O\}]\cdot 4H_2O$ **MeN-Si-1**, and (d) $(Me_2NH_2)_6[\alpha_2\text{-}P_2W_{17}O_{61}\{(H_2C{=}CHCH_2Si)_2O\}]\cdot 6H_2O$ **MeN-Si-2**.

In general, the disorder-free example in the structure analyses of the inorganic−organic hybrids is only a few.[3f] Since the organic groups grafted on the POM have a tendency to disorder, a number of restrains were required for determination of temperature factors of the organic groups. Nevertheless, the present structure analysis is consistent with other characterization data such as elemental analysis, FTIR, and solution (^1H and ^{13}C) NMR spectra. Thus, the use of many restrains will be justified.

Crystal Data for MeN-Ge-1. $C_{17}H_{63}GeN_7O_{64}P_2W_{17}$; M = 4649.72, triclinic, space group $P\bar{1}$, a = 13.35(5), b = 13.36(5), c = 25.66(10) Å, $\alpha = 75.15(6)°$, $\beta = 88.62(6)°$, $\gamma = 68.40(6)°$, V = 4100(3) $Å^3$, Z = 2, $D_{calcd.}$ = 3.766 Mg m^{-3}, μ = 24.235 mm^{-1}, 69450 reflections collected, 20216 independent (R_{int} = 0.0477), R_1 = 0.0434, wR_2 = 0.1300 for $I > 2\sigma(I)$, R_1 = 0.0608, wR_2 = 0.1628, GOF = 1.036 for all data.

As to composition, 6 Me_2NH_2 cations, 1 hydrated water molecule, and polyoxoanion **Ge-1** consisting of 17 tungsten atoms, 2 phosphorus atoms, 63 oxygen atoms, 1 germanium atom, and 3 carbon atoms per formula unit were identified, but the location of 1 Me_2NH_2 cation per formula unit was not determined as a result of disorder.

Crystal Data for MeN-Ge-2. $C_{17}H_{69}N_7O_{65}P_2GeW_{17}$; M = 4671.77, orthorhombic, space group *Pnma*, a = 26.3455(19), b = 20.5810(15), c = 15.0517(11) Å V = 8161.3(10) $Å^3$, Z = 4, $D_{calcd.}$ = 3.802 Mg m^{-3}, μ = 24.353 mm^{-1}, 75947 reflections collected, 10415 independent (R_{int} = 0.0575), R_1 = 0.0532, wR_2 = 0.1348 for $I > 2\sigma(I)$,

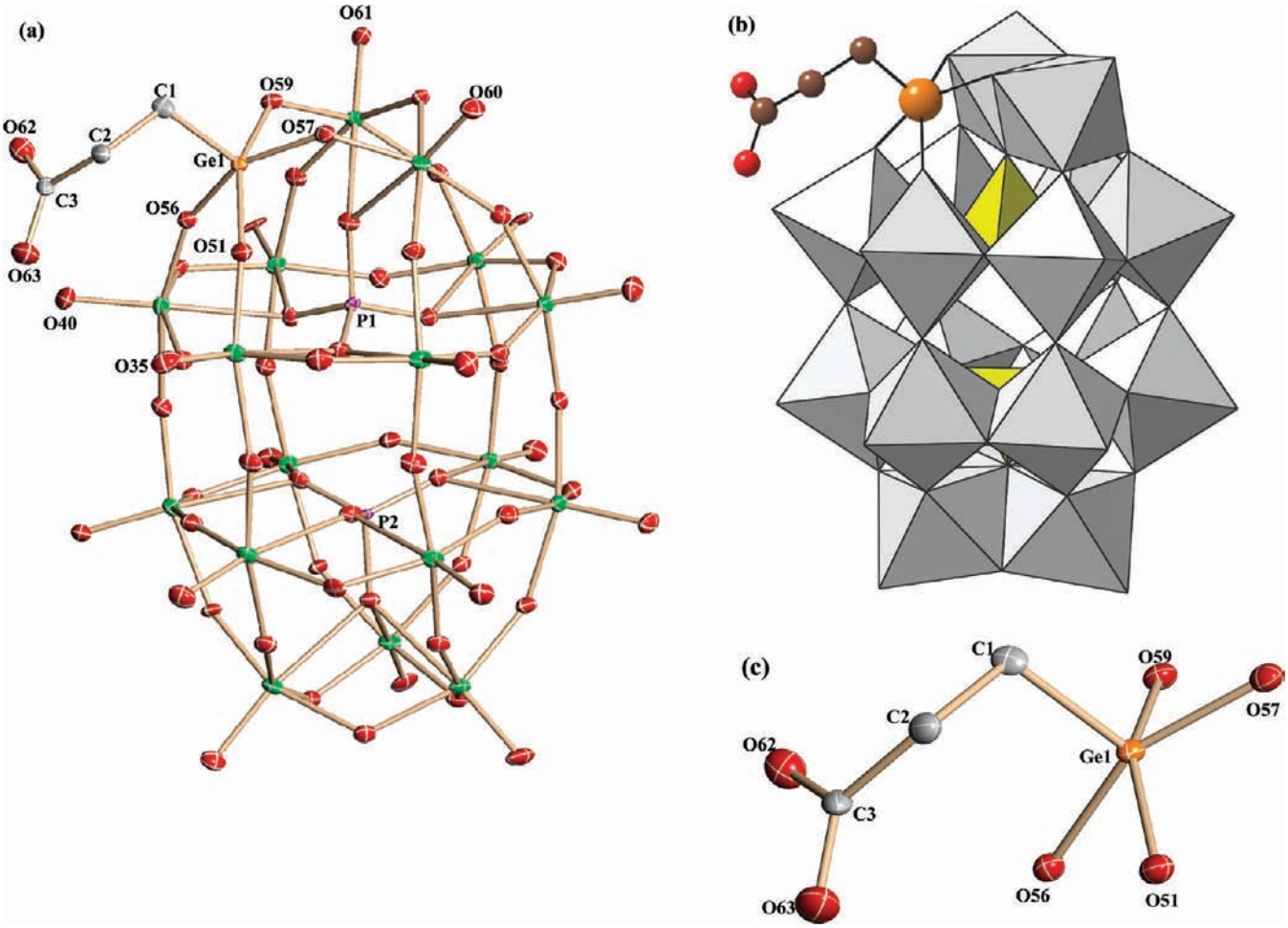

Figure 2. (a) Molecular structure of the polyoxoanion $[\alpha_2\text{-}P_2W_{17}O_{61}(HOOC(CH_2)_2Ge)]^{7-}$ **Ge-1** in **MeN-Ge-1**, (b) its polyhedral representation, and (c) the partial structure around the organogermyl group supported by the polyoxoanion. In (b), the 17 WO_6 and the 2 internal PO_4 groups are shown in gray and yellow, respectively, and the organic groups connected by Ge−O bonds are shown as Ge (orange), O (red), and C (brown) atoms.

R_1 = 0.0640, wR_2 = 0.1416, GOF = 1.127 for all data. A disorder treatment was applied to this compound.

As to composition, 3 Me_2NH_2 cations, 2 hydrated water molecules, and polyoxoanion **Ge-2** consisting of 17 tungsten atoms, 2 phosphorus atoms, 61 oxygen atoms, 1 germanium atom, and 3 carbon atoms per formula unit were identified, but the location of 4 Me_2NH_2 cations and 2 hydrated water molecules per formula unit was not determined as a result of disorder.

Crystal Data for MeN-Si-1. $C_{18}H_{66}N_6O_{70}P_2Si_2W_{17}$; M = 4730.34, monoclinic, space group $P2(1)/n$, a = 24.057(15), b = 13.434(8), c = 26.756(17) Å, β = 107.783(10)°, V = 8233.9(9) Å^3, Z = 4, $D_{calcd.}$ = 3.816 Mg m^{-3}, μ = 23.818 mm^{-1}, 86342 reflections collected, 20497 independent (R_{int} = 0.0492), R_1 = 0.0447, wR_2 = 0.1172 for $I > 2\sigma(I)$, R_1 = 0.0526, wR_2 = 0.1251, GOF = 1.134 for all data.

As to composition, 4 Me_2NH_2 cations, 3 hydrated water molecules, and polyoxoanion **Si-1** consisting of 17 tungsten atoms, 2 phosphorus atoms, 66 oxygen atoms, 2 silicon atoms, and 6 carbon atoms per formula unit were identified, but the location of 2 Me_2NH_2 cations and 1 hydrated water molecule per formula unit was not determined as a result of disorder.

Crystal Data for MeN-Si-2. $C_{36}H_{140}N_{12}O_{136}Si_4P_4W_{34}$; M = 9404.30, triclinic, space group $P\bar{1}$, a = 13.284(3), b = 25.075(5), c = 26.170(5) Å, α = 68.08(3)°, β = 88.92(6)°, γ = 76.63(3)°, V = 7846(3) Å^3, Z = 2, $D_{calcd.}$ = 3.966 Mg m^{-3}, μ = 24.990 mm^{-1}, 70133 reflections collected, 22567 independent (R_{int} = 0.0472), R_1 = 0.0384, wR_2 = 0.0993 for $I > 2\sigma(I)$, R_1 = 0.0466, wR_2 = 0.1049, GOF = 1.033 for all data.

As to composition, 7 Me_2NH_2 cations, 7 hydrated water molecules, and polyoxoanion **Si-2** consisting of 34 tungsten atoms, 4 phosphorus atoms, 124 oxygen atoms, 4 silicon atoms, and 12 carbon atoms per formula unit were identified, but the location of 5 Me_2NH_2 cations and 5 hydrated water molecules per formula unit was not determined as a result of disorder.

CCDC reference numbers 824707 (formula/code: yka015s) for **MeN-Ge-1**, 824708 (formula/code: yto008s) for **MeN-Ge-2**, 824709 (formula/code:mn002mono) for **MeN-Si-1**, and 824710 (yto001bs-tri) for **MeN-Si-2** contain the supplementary crystallographic data for this paper. These data can be obtained free of charge at www.ccdc.cam.ac.uk/conts/retrieving.html (or from Cambridge Crystallographic Data Centre, 12 Union Road, Cambridge CB2 1EZ, U.K.; Fax: +44−1223−336−033; E-mail: deposite@ccdc.cam.ac.uk.)

RESULTS AND DISCUSSION

Synthesis and Compositional Characterization. Dimethylammonium salts of the 1:1 complex of a monolacunary Dawson POM unit: the organic group, that is, the two organogermyl complexes, $(Me_2NH_2)_7[\alpha_2\text{-}P_2W_{17}O_{61}(R_1Ge)]\cdot H_2O$ **MeN-Ge-1** and $(Me_2NH_2)_7[\alpha_2\text{-}P_2W_{17}O_{61}(R_2Ge)]\cdot 4H_2O$ **MeN-Ge-2** (R_1 = $HOOC(CH_2)_2-$ and R_2 = $H_2C{=}CHCH_2-$), were obtained as analytically pure crystals, in 22.8% and 55.3% yields,

dx.doi.org/10.1021/ic201336v |*Inorg. Chem.* 2011, 50, 9606–9619

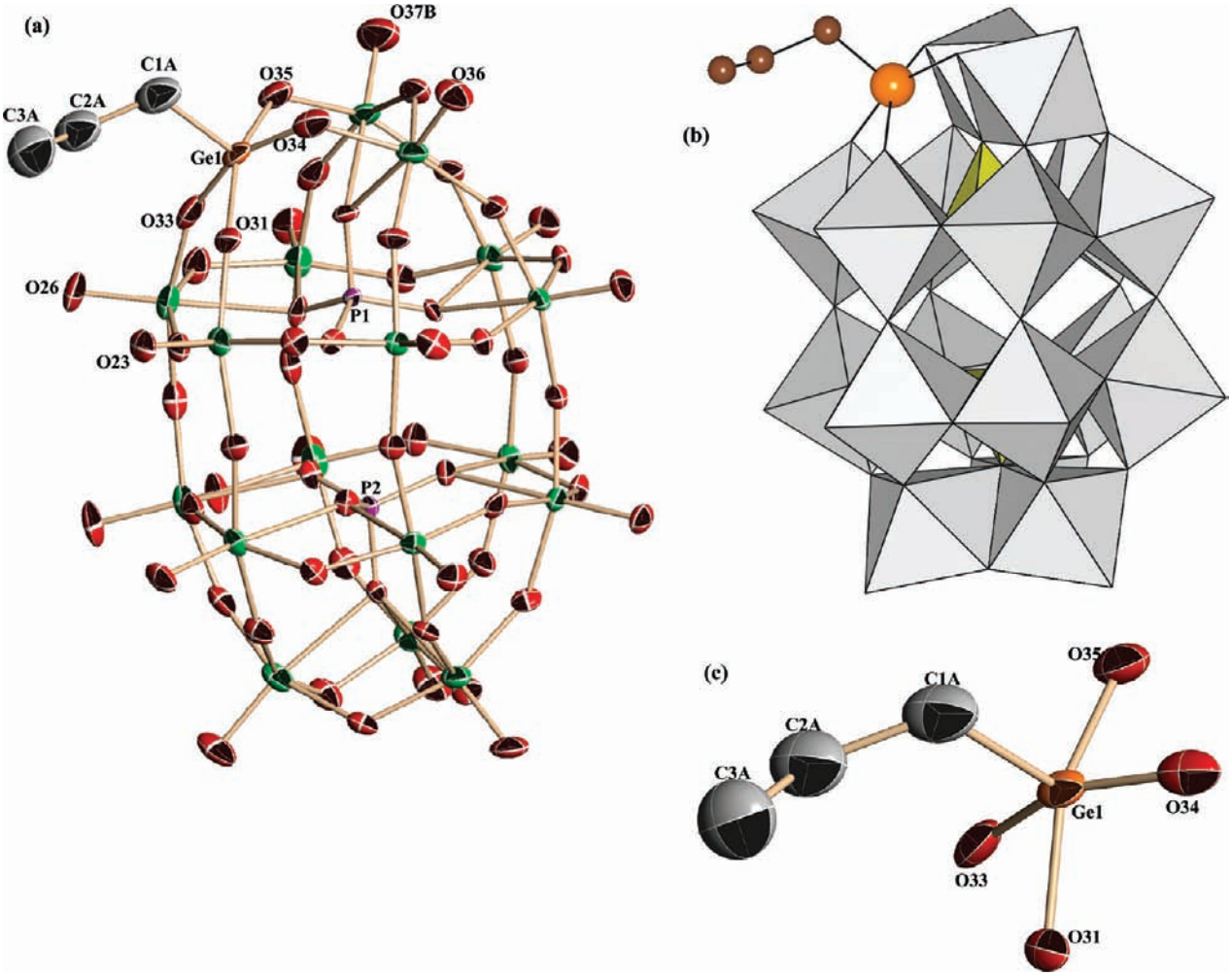

Figure 3. (a) Molecular structure of the polyoxoanion $[\alpha_2\text{-}P_2W_{17}O_{61}(H_2C{=}CHCH_2Ge)]^{7-}$ **Ge-2** in **MeN-Ge-2**, (b) its polyhedral representation, and (c) the partial structure around the organogermyl group supported by the polyoxoanion. In (b), the 17 WO_6 and the 2 internal PO_4 groups are shown in gray and yellow, respectively, and the organic groups connected by Ge−O bonds are shown as Ge (orange) and C (brown) atoms.

by the stoichiometric reactions of $[\alpha_2\text{-}P_2W_{17}O_{61}]^{10-}$ with R_1GeCl_3 in water and R_2GeCl_3 in a solvent mixture of water/acetonitrile, respectively.

The formation of polyoxoanions **Ge-1** and **Ge-2** can be represented in eq 1:

$$RGeCl_3\ (R_1 = HOOC(CH_2)_2^-\ \text{and}\ R_2 = H_2C{=}CHCH_2^-) + [\alpha_2\text{-}P_2W_{17}O_{61}]^{10-} \rightarrow [\alpha_2\text{-}P_2W_{17}O_{61}(RGe)]^{7-}(\textbf{Ge-1},\ R_1\ \text{and}\ \textbf{Ge-2},\ R_2) + 3Cl^- \quad (1)$$

On the other hand, dimethylammonium salts of the 1:2 complex of a monolacunary Dawson POM unit: the organic group, that is, the two organosilyl complexes, $(Me_2NH_2)_6[\alpha_2\text{-}P_2W_{17}O_{61}\text{-}\{(R_1Si)_2O\}]\cdot 4H_2O$ **MeN-Si-1** and $(Me_2NH_2)_6[\alpha_2\text{-}P_2W_{17}O_{61}\text{-}\{(R_2Si)_2O\}]\cdot 6H_2O$ **MeN-Si-2**, were also obtained as analytically pure crystalline crystals, in 17.1% and 63.5% yields, respectively. These compounds were formed by a 1:2 molar ratio reaction of $[\alpha_2\text{-}P_2W_{17}O_{61}]^{10-}$ with $NaOOC(CH_2)_2Si(OH)_2(ONa)$, followed by adjusting pH at <0.5 with aqueous HCl, and by the stoichiometric reaction of $[\alpha_2\text{-}P_2W_{17}O_{61}]^{10-}$ with $H_2C{=}CHCH_2Si(OEt)_3$, followed by adjusting pH at 1.5 with aqueous HCl.

The formation of polyoxoanions **Si-1** and **Si-2** can be represented in eqs 2 and 3, respectively:

$$2NaOOC(CH_2)_2Si(OH)_2(ONa) + [\alpha_2\text{-}P_2W_{17}O_{61}]^{10-} + 8H^+ \rightarrow [\alpha_2\text{-}P_2W_{17}O_{61}\{(R_1Si)_2O\}]^{6-}(\textbf{Si-1}) + 4Na^+ + 4H_2O \quad (2)$$

$$2R_2Si(OEt)_3 + [\alpha_2\text{-}P_2W_{17}O_{61}]^{10-} + 4H^+ + H_2O \rightarrow [\alpha_2\text{-}P_2W_{17}O_{61}\{(R_2Si)_2O\}]^{6-}(\textbf{Si-2}) + 6EtOH \quad (3)$$

The composition and formulas of **MeN-Ge-1**, **MeN-Ge-2**, **MeN-Si-1**, and **MeN-Si-2** were consistent with CHN elemental analysis, TG/DTA, FTIR, solid-state CPMAS ^{31}P NMR and solution (^{31}P, ^1H and ^{13}C) NMR spectroscopy, and X-ray crystallography. As to the stability in the solid state, decomposition began at around 153 °C for **MeN-Ge-1**, at around 143 °C for **MeN-Ge-2**, at around 230 °C for **MeN-Si-1**, and at around 119 °C for **MeN-Si-2**.

As shown in X-ray crystallography, a siloxane bond (Si−O−Si bond) was formed in **Si-1** and **Si-2**, whereas a Ge−O−Ge bond was not formed in **Ge-1** and **Ge-2**. In the crystals of **MeN-Si-2**, two complexes with different orientations of two organic groups

dx.doi.org/10.1021/ic201336v |*Inorg. Chem.* 2011, 50, 9606–9619

Table 1. Selected Bond Lengths (Å) and Angles (deg) around the Germanium Site in Ge-1

Bond Lengths/Å			
C(1)−Ge(1)	1.895(13)	Ge(1)−O(51)	1.895(9)
C(1)−C(2)	1.531(18)	Ge(1)−O(56)	1.888(9)
C(2)−C(3)	1.501(18)	Ge(1)−O(57)	1.871(9)
C(3)−O(62)	1.262(16)	Ge(1)−O(59)	1.876(9)
C(3)−O(63)	1.298(16)		
Bond Angles/deg			
C(2)−C(1)−Ge(1)	115.1(9)	O(59)−Ge(1)−C(1)	103.8(5)
C(3)−C(2)−C(1)	115.5(11)	O(51)−Ge(1)−O(57)	88.3(4)
O(62)−C(3)−C(2)	122.3(12)	O(51)−Ge(1)−O(59)	152.2(4)
O(63)−C(3)−C(2)	115.7(12)	O(57)−Ge(1)−O(59)	86.7(4)
O(62)−C(3)−O(63)	122.0(12)	O(51)−Ge(1)−O(56)	84.5(4)
O(51)−Ge(1)−C(1)	104.0(5)	O(57)−Ge(1)−O(56)	153.8(4)
O(56)−Ge(1)−C(1)	103.2(5)	O(59)−Ge(1)−O(56)	88.1(4)
O(57)−Ge(1)−C(1)	103.0(5)		

Table 2. Selected Bond Lengths (Å) and Angles (deg) around the Germanium Site in Ge-2

Bond Lengths/Å			
C(1A)−Ge(1)	1.92(5)	Ge(1)−O(35)	1.870(8)
C(1A)−C(2A)	1.60(15)	Ge(1)−O(33)	1.891(14)
C(2A)−C(3A)	1.34(7)	Ge(1)−O(31)	1.922(10)
Ge(1)−O(34)	1.859(14)		
Bond Angles/deg			
C(2A)−C(1A)−Ge(1)	116(8)	O(34)−Ge(1)−O(35)	89.9(7)
C(3A)−C(2A)−C(1A)	130(8)	O(34)−Ge(1)−O(33)	157.3(5)
C(1A)−Ge(1)−O(31)	100(4)	O(35)−Ge(1)−O(33)	88.8(7)
O(33)−Ge(1)−C(1A)	103(5)	O(34)−Ge(1)−O(31)	87.3(5)
O(34)−Ge(1)−C(1A)	99(5)	O(35)−Ge(1)−O(31)	156.7(5)
O(35)−Ge(1)−C(1A)	103(4)	O(33)−Ge(1)−O(31)	84.9(5)

were found, designated as A-type and B-type complexes, the difference of which was found only by X-ray crystallography (see molecular structures of **Si-1** and **Si-2**).

The Si-containing compounds were formed under strongly acidic conditions, while the Ge-containing compounds were formed without addition of any acids. So far, many inorganic−organic hybrid compounds connected with two organic groups by a siloxane bond have been found in Keggin and Dawson POM-families.[2−8] On the other hand, only one example of Dawson POM-based organogermyl complexes is known; the reactions of α_2-monolacunary Dawson POMs with GeX_4 (X = OEt, Cl) gave crystals of a monogermanium-substituted Dawson POM, $(Me_2NH_2)_7[\alpha_2\text{-}P_2W_{17}O_{61}(GeOH)]\cdot 5H_2O$, although the Ge site was not determined due to disorder of the α-Dawson structure.[6e] Even when excess amounts of GeX_4 were used for the constant amount of $[\alpha_2\text{-}P_2W_{17}O_{61}]^{10-}$, only a 1:1 complex was obtained.

The FTIR spectra (Figure 1) of **MeN-Ge-1**, **MeN-Ge-2**, **MeN-Si-1**, and **MeN-Si-2**, measured in KBr disks, showed the characteristic bands due to the Dawson POM framework (1086, 953, 924, and 771 cm^{-1} for **MeN-Ge-1** and 1087, 953, 920, and 769 cm^{-1} for **MeN-Ge-2**; 1088, 957, 925, and 797 cm^{-1} for **MeN-Si-1** and 1089, 955, 921, and 796 cm^{-1} for **MeN-Si-2**).[10] The IR spectral patterns of **MeN-Si-1** and **MeN-Si-2** were similar to those of inorganic−organic hybrid compounds with siloxane bonds, such as $[\alpha_2\text{-}P_2W_{17}O_{61}\{(RSi)_2O\}]^{6-}$ (R = $HS(CH_2)_3-$, $NCS(CH_2)_3-$, and $Me_3N^+(CH_2)_3-$[6c]) and (R = $\{H_2C{=}C(CH_3)OCO(CH_2)_3-\}$, $\{H_2C{=}CHOCO(CH_2)_3-\}$, and $\{H_2C{=}CH-\}$[6d]).

The Si−O−Si vibrational bands overlapped with the P−O vibrational bands, while the former bands have been found as intense bands at around 1111 and 1121 cm^{-1} in the inorganic−organic hybrids of Keggin POMs.[5p]

In **Ge-1** and **Si-1**, the presence of terminal −COOH groups was confirmed by IR bands at 1705 cm^{-1} for **Ge-1** and at 1728 cm^{-1} for **Si-1**. In **Ge-2** and **Si-2**, the terminal C=C vibrational bands overlapped with the O−H bands of water molecules. The C=O and C=C vibrational bands have been observed at 1702 and 1629 cm^{-1}, respectively, for R = $\{H_2C{=}C(CH_3)COO(CH_2)_3-\}$ in $[\alpha_2\text{-}P_2W_{17}O_{61}\{(RSi)_2O\}]^{6-}$ and at 1713 and 1616 cm^{-1}, respectively, for R = $\{H_2C{=}CHCOO(CH_2)_3-\}$.[6d]

Molecular Structures of Ge-1 and Ge-2. The molecular structures of **Ge-1** and **Ge-2** revealed that one organic chain was supported in the monolacunary site of the Dawson POM $[\alpha_2\text{-}P_2W_{17}O_{61}]^{10-}$ (Figures 2a and 3a), in contrast to the two organic chains supported in the monolacunary sites in **Si-1** and **Si-2**. Their polyhedral representations are shown in Figures 2b and 3b, and the partial structures around the siloxane bonds are shown in Figures 2c and 3c. A disorder treatment was applied to the structure analysis of **Ge-2**.

Each Ge atom in the organogermyl group exhibited five coordination with the terminal organic group R and four oxygen atoms in the lacunary sites of the POMs: (O56, O59, O51, and O57) in **Ge-1** (Figure 2c) and (O34, O35, O33, and O31) in **Ge-2** (Figure 3c).

The bond lengths of Ge−O (oxygen atoms in the lacunary site) were in the range of 1.871(9)−1.895(9) Å (average, 1.883 Å) for **Ge-1** (Table 1) and 1.859(14)−1.922(10) Å (average, 1.886 Å) for **Ge-2** (Table 2); these bond lengths were longer than those of Si−O for **Si-1** (average 1.64 Å) (Table 3), those of Si−O for **Si-2** (average 1.625 Å (B-type) and 1.633 Å (A-type) (Table 4), and those of Si−O for other related organosilyl compounds. The C(2)−C(1)−Ge(1) angle (115.1(9)°) in **Ge-1** was similar to the C(2A)-C(1A)-Ge(1) angle (116(8)°) in **Ge-2**.

As to the terminal −COOH group in the organic chain, the bond lengths and angle (C(3)−O(62) 1.262(16) Å and C(3)−O(63) 1.298(16) Å, O(62)−C(3)−O(63) 122.0(12)°) in **Ge-1** can be compared with those in **Si-1** (average 1.27 Å and 121.5°). Pope et al. have previously reported $[PW_{11}O_{39}RhCH_2COOH]^{5-}$, $[SiW_{11}O_{39}RhCH_2COOH]^{6-}$, and $[\alpha_2\text{-}P_2W_{17}O_{61}RhCH_2COOH]^{8-}$,[3c] as the complex carrying one terminal functional group that can be further derivatized. As a matter of fact, they have synthesized the amide derivative $[PW_{11}O_{39}RhCH_2CONHPh]^{5-}$ by a standard procedure.

As to the allyl group in the organic chain, the C−C bond length in the organogermyl group in **Ge-2** (C(2A)−C(3A) 1.34(7) Å) and those in the organosilyl groups in **Si-2** (C(2BR)−C(3BR) 1.05(3) Å and C(2BL)−C(3BL) 1.30(2) Å for B-type; C(2AR)−C(3AR) 1.21(3) Å and C(2AL)−C(3AL) 1.25(3) Å for A-type) indicated a double-bond character, which can be compared with those of $[\alpha_2\text{-}P_2W_{17}O_{61}\{(RSi)_2O\}]^{6-}$ (C(5)−C(6) 1.42(4) Å and C(13)−C(14)

dx.doi.org/10.1021/ic201336v |*Inorg. Chem.* 2011, 50, 9606–9619

Table 3. Selected Bond Lengths (Å) and Angles (deg) around the Siloxane Bond in Si-1

Bond Lengths/Å			
C(1R)−Si(1)	1.85(5)	C(1 L)−Si(2)	1.84(5)
C(1R)−C(2R)	1.52(7)	C(1 L)−C(2 L)	1.51(9)
C(2R)−C(3R)	1.50(7)	C(2 L)−C(3 L)	1.41(16)
C(3R)−O(63R)	1.23(7)	C(3 L)−O(63 L)	1.07(15)
C(3R)−O(64R)	1.32(7)	C(3 L)−O(64 L)	1.45(16)
O(60)−Si(1)	1.63(3)	O(60)−Si(2)	1.64(3)
O(51)−Si(1)	1.62(3)	O(56)−Si(2)	1.63(3)
O(57)−Si(1)	1.66(3)	O(59)−Si(2)	1.63(3)
Bond Angles/deg			
C(2R)−C(1R)−Si(1)	115(4)	C(2 L)−C(1 L)−Si(2)	117(4)
C(3R)−C(2R)−C(1R)	114(4)	C(3 L)−C(2 L)−C(1 L)	117(8)
C(2R)−C(3R)−O(63R)	125(5)	C(2 L)−C(3 L)−O(63 L)	132(10)
C(2R)−C(3R)−O(64R)	110(5)	C(2 L)−C(3 L)−O(64 L)	109(10)
O(64R)−C(3R)−O(63R)	125(5)	C(64 L)−C(3 L)−O(63 L)	118(10)
O(60)−Si(1)−C(1R)	109(2)	O(60)−Si(2)−C(1 L)	109(2)
O(51)−Si(1)−C(1R)	111(2)	O(56)−Si(2)−C(1 L)	111(2)
O(57)−Si(1)−C(1R)	113(2)	O(59)−Si(2)−C(1 L)	112(2)
O(51)−Si(1)−O(57)	108.6(17)	O(56)−Si(2)−O(59)	108.9(17)
O(51)−Si(1)−O(60)	109.7(17)	O(56)−Si(2)−O(60)	108.6(17)
O(60)−Si(1)−O(57)	106.0(17)	O(59)−Si(2)−O(60)	106.4(17)
		Si(1)−O(60)−Si(2)	127(2)

1.39(4) Å for R = {H_2C═$C(CH_3)COO(CH_2)_3$−}; C(5)−C(6) 1.33(4) Å and C(11)−C(12) 1.38(4) Å for R = {H_2C═$CHCOO(CH_2)_3$−}).[6d]

The W−O bond lengths (terminal oxygen) in the lacunary site were in the range of 1.716(10)−1.734(9) Å (average 1.725 Å) in **Ge-1** (Supporting Information, Table S1), 1.711-(11)−1.718(10) Å (average 1.715 Å) in **Ge-2** (for 3 oxygen atoms except O(37B)) (Supporting Information, Table S2), 1.70(3)−1.72(3) Å (average 1.71 Å) in **Si-1** (Supporting Information, Table S3) and 1.686(11)−1.721(10) Å (average 1.707 Å) in **Si-2** (A-type); 1.692(9)−1.719(10) Å (average 1.707 Å) in **Si-2** (B-type) (Supporting Information, Table S4). These bond lengths were almost the same as those of W−O (terminal oxygen) in the lacunary site in $[\alpha_2\text{-}P_2W_{17}O_{61}]^{10-}$ (ca. 1.7 Å),[6a] but shorter than those of $[\alpha_2\text{-}P_2W_{17}O_{61}\text{-}\{(RSi)_2O\}]^{6-}$ (1.868−1.914 Å for R = {H_2C═$C(CH_3)COO(CH_2)_3$−}; 1.875−1.920 Å for R = {H_2C═$CHCOO(CH_2)_3$−}).[6d]

On the other hand, the W−O bond lengths in the W_3 cap and the two W_6 belts, that is, W−O_t (O_t; terminal oxygen), W−O_c (O_c; corner-sharing oxygen), W−O_e (O_e; edge-sharing oxygen), and W−O_a (O_a; oxygen coordinated to a P atom) (Supporting Information, Tables S1−S4), were in the normal range.[1,6a]

For **Ge-1** (Supporting Information, Table S5), the bond valence sums (BVS)[11] of the 17 W atoms, calculated on the basis of the observed bond lengths, were in the range of 5.875−6.259 (average 6.082), those of the two P atoms were 4.829−4.909 (average 4.869), and that of the Ge atom was 4.372. The BVS values of the 61 O atoms were in the range of 1.640−2.141 (average 1.903). However, the BVS values of O(62) and O(63) in the terminal −COOH group were not estimated because of a disorder. These BVS values correspond reasonably well to the formal valences W^{6+}, P^{5+}, Ge^{4+}, and O^{2-}, respectively. On the other hand, for **Ge-2** (Supporting Information, Table S6), the BVS values of the W, P, and O atoms correspond to their formal valences W^{6+}, P^{5+}, and O^{2-}, respectively, but those of the W(10), Ge, and O(37B) atoms were not estimated because of a disorder.

Molecular Structures of Si-1 and Si-2. The molecular structures of **Si-1** and **Si-2** revealed that the two organic chains connected by an Si−O−Si bond were supported in the monolacunary site of the Dawson POM $[\alpha_2\text{-}P_2W_{17}O_{61}]^{10-}$ (Figures 4a, 5a, and 6a). Their polyhedral representations are shown in Figures 4b, 5b, and 6b, and the partial structures around the siloxane bonds are shown in Figures 4c, 5c, and 6c. The precision of the bond lengths and angles in **Si-1** were lowered because of a disorder treatment (Table 3). In the crystals of **MeN-Si-2**, two complexes based on different orientations of two organic groups were found, designated as B-type (Figure 5) and A-type (Figure 6). In the B-type complex, both lines passing through the C1BR/C2BR atoms and the C1BL/C2BL atoms are almost parallel to the plane formed by the O59B, O56B, O57B, and O51B atoms. On the other hand, in the A-type complex, a line passing through the C1AR and C2AR atoms intersects the plane formed by O59A, O56A, O57A, and O51A atoms at (almost) a right angle, while a line passing through the C1AL and C2AL atoms is almost parallel to the plane (Figure 6c).

As to the two organic chains in **Si-1** (Figure 4a), the bond angle and lengths of (C(2R)−C(1R)−Si(1) 115(4)°, C(1R)−Si(1) 1.85(5) Å, O(60)−Si(1) 1.63(3) Å) in one chain were almost the same as those of (C(2L)−C(1L)−Si(2) 117(4)°, C(1L)−Si(2) 1.84(5) Å, O(60)−Si(2) 1.64(3) Å) in the other chain (Table 3). If the terminal −COOH groups are ignored, the POM molecule of **Si-1** in the solid state is represented as an approximate C_s symmetry compound. On the other hand, if the terminal C atoms are ignored, the two

dx.doi.org/10.1021/ic201336v |*Inorg. Chem.* 2011, 50, 9606–9619

Table 4. Selected Bond Lengths (Å) and Angles (deg) around the Siloxane Bond in Si-2

B-Type Complex Bond Lengths/Å			
C(1BR)−Si(1B)	1.856(16)	C(1BL)−Si(2B)	1.841(15)
C(1BR)−C(2BR)	1.47(3)	C(1BL)−C(2BL)	1.50(2)
C(2BR)−C(3BR)	1.05(3)	C(2BL)−C(3BL)	1.30(2)
O(60B)−Si(1B)	1.635(10)	O(60B)−Si(2B)	1.612(10)
O(51B)−Si(1B)	1.635(10)	O(56B)−Si(2B)	1.624(10)
O(57B)−Si(1B)	1.620(11)	O(59B)−Si(2B)	1.619(10)
B-Type Complex Bond Angles/deg			
C(2BR)−C(1BR)−Si(1B)	114.7(13)	C(2BL)−C(1BL)−Si(2B)	113.1(11)
C(3BL)−C(2BL)−C(1BL)	124.8(16)	C(3BL)−C(2BL)−C(1BL)	124.8(16)
O(60B)−Si(1B)−C(1BR)	109.8(6)	O(60B)−Si(2B)−C(1BL)	110.9(6)
O(51B)−Si(1B)−C(1BR)	111.3(6)	O(56A)−Si(2A)−C(1AL)	109.4(6)
O(57B)−Si(1B)−C(1BR)	110.6(6)	O(56B)−Si(2B)−C(1BL)	107.8(6)
O(57B)−Si(1B)−O(51B)	108.3(5)	O(59B)−Si(2B)−O(56B)	109.0(5)
O(60B)−Si(1B)−O(51B)	108.0(5)	O(60B)−Si(2B)−O(56B)	107.7(5)
O(57B)−Si(1B)−O(60B)	108.8(5)	O(60B)−Si(2B)−O(59B)	108.6(5)
		Si(2B)−O(60B)−Si(1B)	128.7(6)
A-Type Complex Bond Lengths/Å			
C(1AR)−Si(1A)	1.851(15)	C(1AL)−Si(2A)	1.836(16)
C(1AR)−C(2AR)	1.52(2)	C(1AL)−C(2AL)	1.49(2)
C(2AR)−C(3AR)	1.21(3)	C(2AL)−C(3AL)	1.25(3)
O(60A)−Si(1A)	1.625(11)	O(60A)−Si(2A)	1.633(10)
O(51A)−Si(1A)	1.634(10)	O(56A)−Si(2A)	1.619(10)
O(57A)−Si(1A)	1.634(10)	O(59A)−Si(2A)	1.644(11)
A-Type Complex Bond Angles/deg			
C(2AR)−C(1AR)−Si(1A)	110.4(11)	C(2AL)−C(1AL)−Si(2A)	116.2(12)
C(3AR)−C(2AR)−C(1AR)	129(2)	C(3AL)−C(2AL)−C(1AL)	130(2)
O(60A)−Si(1A)−C(1AR)	109.7(6)	O(60A)−Si(2A)−C(1AL)	110.1(6)
O(51A)−Si(1A)−C(1AR)	111.1(6)	O(56A)−Si(2A)−C(1AL)	109.4(6)
O(57A)−Si(1A)−C(1AR)	109.5(6)	O(59A)−Si(2A)−C(1AL)	112.5(6)
O(57A)−Si(1A)−O(51A)	109.2(5)	O(56A)−Si(2A)−O(59A)	109.8(5)
O(60A)−Si(1A)−O(51A)	108.4(5)	O(56A)−Si(2A)−O(60A)	107.7(5)
O(60A)−Si(1A)−O(57A)	108.8(5)	O(60A)−Si(2A)−O(59A)	107.3(5)
		Si(1A)−O(60A)−Si(2A)	129.4(6)

organic chains in **Si-2** (B-type) are almost symmetrically oriented within the plane containing the Si−O−Si bond (Figure 5a): the bond angle and lengths of (C(2BR)−C(1BR)−Si(1B) 114.7(13)°, C(1BR)−Si(1B) 1.856(16) Å, O(60B)−Si(1B) 1.635(10) Å) in one chain were approximately the same as those of (C(2BL)−C(1BL)−Si(2B) 113.1(11)°, C(1BL)−Si(2B) 1.841(15) Å, O(60B)−Si(2B) 1.612(10) Å) in the other chain (Table 4). Thus, this POM molecule in the solid state can also be depicted as an approximate C_s symmetry compound. These features can be compared with the symmetry of related POM-based organosilyl complexes in the solid state: $[\alpha_2\text{-}P_2W_{17}O_{61}\{(RSi)_2O\}]^{6-}$ (R = Ph;[6a] R = $\{H_2C{=}CHCOO(CH_2)_3-\}$[6d]), both with C_s symmetry.

Each Si atom in the organosilyl groups exhibited four-coordination with the terminal organic group R, one bridging oxygen atom in the Si−O−Si bond, and two of the four oxygen atoms in the lacunary sites of the POMs (Figures 4c, 5c, and 6c); (O56, O59, O51, and O57) in **Si-1**, (O56B, O59B, O51B, and O57B) in **Si-2** (B-type), and (O56A, O59A, O51A, and O57A) in **Si-2** (A-type).

The bond lengths of Si−O (oxygen atoms in the lacunary site) were in the range 1.62−1.66 Å (average 1.64 Å) for **Si-1**, 1.619−1.635 Å (average 1.625 Å) for **Si-2** (B-type), and 1.619−1.644 Å (average 1.633 Å) for **Si-2** (A-type); these bond lengths can be compared with those of related POMs, $[\alpha_2\text{-}P_2W_{17}O_{61}\{(HSC_3H_6Si)_2O\}]^{6-}$ (1.611−1.650 Å), $[\alpha_2\text{-}P_2W_{17}O_{61}\{(NCSC_3H_6Si)_2O\}]^{6-}$ (1.608−1.647 Å), $[\alpha_2\text{-}P_2W_{17}O_{61}\{(PhSi)_2O\}]^{6-}$ (1.613−1.651 Å),[6b] and $[\alpha_2\text{-}P_2W_{17}O_{61}\{(RSi)_2O\}]^{6-}$ (1.603−1.641 Å for R = $\{H_2C{=}C(CH_3)COO(CH_2)_3-\}$; 1.626−1.648 Å for R = $\{H_2C{=}CHCOO(CH_2)_3-\}$).[6d]

The bond lengths in the Si−O−Si moieties were Si(1)−O(60) 1.63(3) Å and Si(2)−O(60) 1.64(3) Å for **Si-1**, Si(1B)−O(60B) 1.635(10) Å and Si(2B)−O(60B) 1.612(10) Å for **Si-2** (B-type) and Si(1A)−O(60A) 1.625(11) Å and Si(2A)−O(60A) 1.633(10) Å for **Si-2** (A-type), which were similar to those of $[\alpha_2\text{-}P_2W_{17}O_{61}\{(RSi)_2O\}]^{6-}$ (1.597−1.627 Å for R = $\{H_2C{=}C(CH_3)COO(CH_2)_3-\}$; 1.626−1.643 Å for R = $\{H_2C{=}CHCOO(CH_2)_3-\}$).[6d]

dx.doi.org/10.1021/ic201336v |*Inorg. Chem.* 2011, 50, 9606–9619

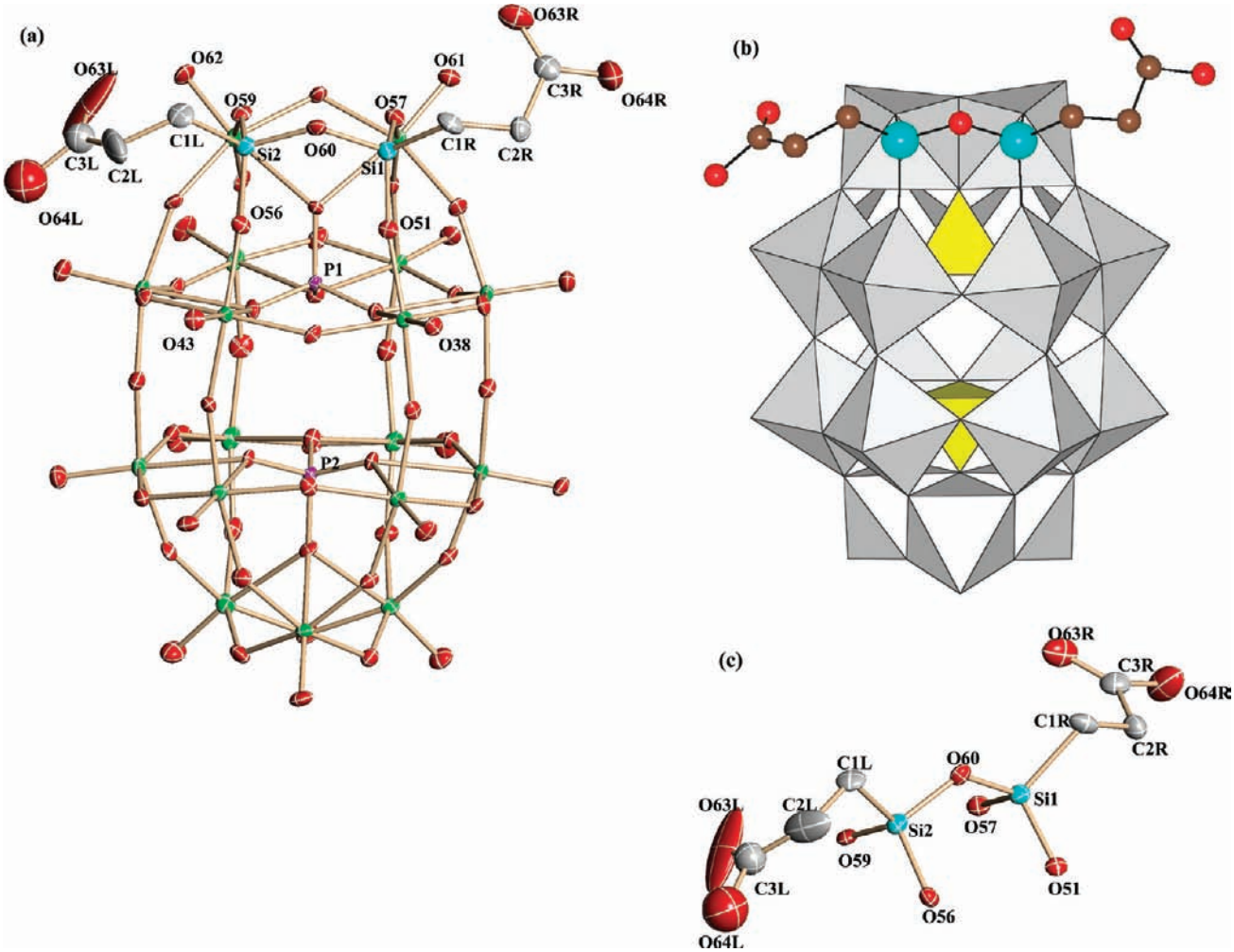

Figure 4. (a) Molecular structure of the polyoxoanion $[\alpha_2\text{-}P_2W_{17}O_{61}\{(HOOC(CH_2)_2Si)_2O\}]^{6-}$ **Si-1** in **MeN-Si-1**, (b) its polyhedral representation, and (c) the partial structure around the siloxane bond supported by the polyoxoanion. In (b), the 17 WO_6 and the 2 internal PO_4 groups are shown in gray and yellow, respectively, and the organic groups connected by a siloxane bond are shown as Si (light blue), O (red), and C (brown) atoms.

The Si−O−Si bond angles in **Si-1** (127(2)°) and **Si-2** (128.7(6)° for B-type and 129.4(6)° for A-type) can be compared with those of $[\alpha_2\text{-}P_2W_{17}O_{61}\{(RSi)_2O\}]^{6-}$ (131.2(10)° for R = $\{H_2C{=}C(CH_3)COO(CH_2)_3{-}\}$; 125.9(11)° for R = $\{H_2C{=}CHCOO(CH_2)_3{-}\}$),[6d] $[\alpha_2\text{-}P_2W_{17}O_{61}\{(HS(CH_2)_3Si)_2O\}]^{6-}$ (126.3)°, $[\alpha_2\text{-}P_2W_{17}O_{61}\{(NCS(CH_2)_3Si)_2O\}]^{6-}$ (124.7)° and $[\alpha_2\text{-}P_2W_{17}O_{61}\{(PhSi)_2O\}]^{6-}$ (127.4)°.[6b]

As shown in Tables S7 and S8 of the Supporting Information, the bond valence sums (BVS)[11] of the 17 W atoms were in the range of 6.064−6.255 (average 6.179) for **Si-1**, 5.942−6.267 (average 6.151) for **Si-2** (B-type), and 5.953−6.300 (average 6.129) for **Si-2** (A-type); those of the two P atoms were 4.894−4.931 (average 4.913) for **Si-1**, 4.884−4.892 (average 4.888) for **Si-2** (B-type), and 4.855−4.901 (average 4.878) for **Si-2** (A-type); those of the two Si atoms were 4.155−4.211 for **Si-1**, 4.191−4.333 for **Si-2** (B-type), and 4.074−4.107 for **Si-2** (A-type). The BVS values of the 61 O atoms for **Si-1** were in the range of 1.703−2.162 (average 1.957), 1.658−2.162 (average 1.948) for **Si-2** (B-type), and 1.698−2.149 (average 1.939) for **Si-2** (A-type). The BVS values of O(63R), O(63 L), O(64R), and O(64 L) in the two terminal −COOH groups in **Si-1** were not estimated because of a disorder. The BVS values of the oxygen atoms in the siloxane bonds were 2.028 (O(60)) for **Si-1**, 2.093 (O(60B) for **Si-2** (B-type), and 2.060 (O(60A) for **Si-2** (A-type). These BVS values correspond reasonably well to the formal valences W^{6+}, P^{5+}, Si^{4+}, and O^{2-}, respectively.

Solid-State CPMAS ^{31}P NMR and Solution (^{31}P, ^{1}H, ^{13}C) NMR. Solid-state CPMAS ^{31}P NMR (Supporting Information, Figure S1) of the crystalline samples of the dimethylammonium salts showed two broad peaks at −9.5 and −12.9 ppm for **MeN-Ge-1**, −9.6 and −12.7 ppm for **MeN-Ge-2**, −9.5 and −12.7 ppm for **MeN-Si-1**, and −9.9 and −13.1 ppm for **MeN-Si-2**, containing both B-type and A-type complexes. These spectra should correspond to their solid-state structures shown by X-ray crystallography.

On the other hand, solid-state CPMAS ^{13}C NMR spectra of these compounds were tried to measure with SCANS more than 30 000. However, only broad signals due to many dimethylammonium counterions were observed, but the carbon signals due to the organic chains R_1 and R_2 were hidden under the noise.

POMs **Ge-1** and **Ge-2** were stable in H_2O, while POMs **Si-1** and **Si-2** in H_2O had a tendency to produce the monolacunary Dawson POM species by releasing the organic groups (Supporting Information, Figure S2). The ^{31}P NMR in D_2O

dx.doi.org/10.1021/ic201336v |*Inorg. Chem.* 2011, 50, 9606–9619

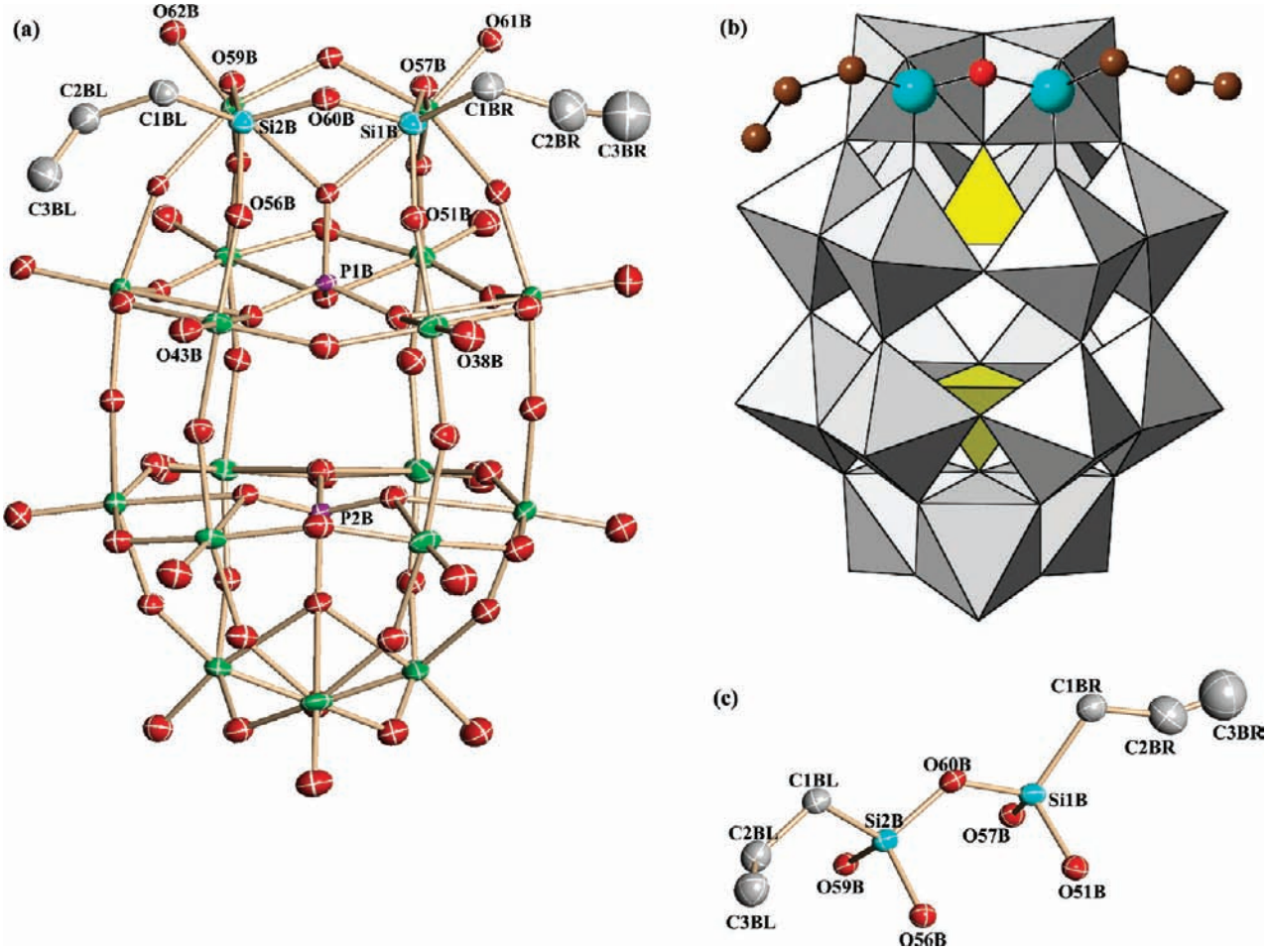

Figure 5. (a) Molecular structure of the polyoxoanion $[\alpha_2\text{-}P_2W_{17}O_{61}\{(H_2C{=}CHCH_2Si)_2O\}]^{6-}$ **Si-2** in **MeN-Si-2** (B-type), (b) its polyhedral representation, and (c) the partial structure around the siloxane bond supported by the polyoxoanion. In (b), the 17 WO_6 and the 2 internal PO_4 groups are shown in gray and yellow, respectively, and the organic groups connected by a siloxane bond are shown as Si (light blue), O (red), and C (brown) atoms.

exhibited a clean two-line spectrum at δ −10.27 and −13.57 for **Ge-1**, and at δ −10.20 and −13.53 for **Ge-2**, thereby confirming their purity and homogeneity. In relation to these facts, $(Me_2NH_2)_7[\alpha_2\text{-}P_2W_{17}O_{61}(GeOH)]\cdot 5H_2O$ exhibited solid-state ^{31}P NMR at δ −10.88 and −13.08 plus solution ^{31}P NMR in D_2O at δ −11.10 and −13.38, showing that the solid-state structure is maintained in solution.[6e]

On the other hand, ^{31}P NMR in D_2O of **Si-1** showed major peaks at δ −10.25 and −13.25 and minor peaks at δ −8.45 and −13.10 due to the monolacunary Dawson POM, and those of **Si-2** showed major peaks at δ −10.28 and −13.30 and minor peaks at δ −8.31 and −13.36 due to the monolacunary Dawson POM. The minor peaks grew as time passed, although their growth stopped three days later after dissolving. The two major ^{31}P NMR peaks in D_2O were very similar to those of $[\alpha_2\text{-}P_2W_{17}O_{61}\{(RSi)_2O\}]^{6-}$ (δ −10.3 and −13.2 for R = $\{H_2C{=}C(CH_3)\text{-}COO(CH_2)_3{-}\}$; δ −10.2 and −13.3 for R = $\{H_2C{=}CHCOO\text{-}(CH_2)_3{-}\}$),[6d] $[\alpha_2\text{-}P_2W_{17}O_{61}\{(HS(CH_2)_3Si)_2O\}]^{6-}$ (δ −10.5, −13.5), $[\alpha_2\text{-}P_2W_{17}O_{61}\{(NCS(CH_2)_3Si)_2O\}]^{6-}$ (δ −10.3, −13.8), and $[\alpha_2\text{-}P_2W_{17}O_{61}\{(PhSi)_2O\}]^{6-}$ (δ −10.2, −13.3).[6b] The terminal functional groups in the organic chains influenced the two ^{31}P NMR signals of the Dawson unit less.

POM **Si-1** is stable in a 6 M aqueous HCl solution, showing a two-line ^{31}P NMR spectrum at δ −10.37 and −13.42 and no other minor peaks (Supporting Information, Figure S2). On the other hand, POM **Si-2**, just after dissolving in a 6 M aqueous HCl solution, showed a two-line ^{31}P NMR spectrum at δ −10.40 and −13.41 (Supporting Information, Figure S2). However, it showed a tendency to release the organic chains as time passed, and in four days after dissolving, it was completely converted to the previously reported, trimeric species formed by siloxane bonds, $[\{\alpha_2\text{-}P_2W_{17}O_{61}(Si_2O)\}_3(\mu\text{-}O)_3]^{18-}$,[6e] which showed ^{31}P NMR at δ −10.13 and −13.30. The trimer formed was also confirmed by X-ray structure analysis. Probably, the allylsilyl groups in **Si-2** under strongly acidic conditions underwent dissociation to produce a reactive monomer unit (RMU), which readily oligomerizes to form the trimer.[6e]

The solution ^{13}C NMR spectra of **Ge-1**, **Ge-2**, **Si-1**, and **Si-2** have shown very small signals due to the organic chains, compared with large signals due to the dimethylammonium counterions. The ^{1}H and ^{13}C NMR signals in D_2O of **Ge-1** and **Ge-2** were assigned, respectively, showing that the organic chains were bound to the POMs in aqueous solutions. The ^{1}H NMR signals in 6 M aqueous DCl and the ^{13}C NMR signals in 6 M aqueous HCl of **Si-1** also showed that the organic chains were bound to the POM. The ^{1}H and ^{13}C NMR signals in D_2O of **Si-2**, just after dissolving, showed the allylsilyl groups bound to the POM.

dx.doi.org/10.1021/ic201336v |*Inorg. Chem.* 2011, 50, 9606–9619

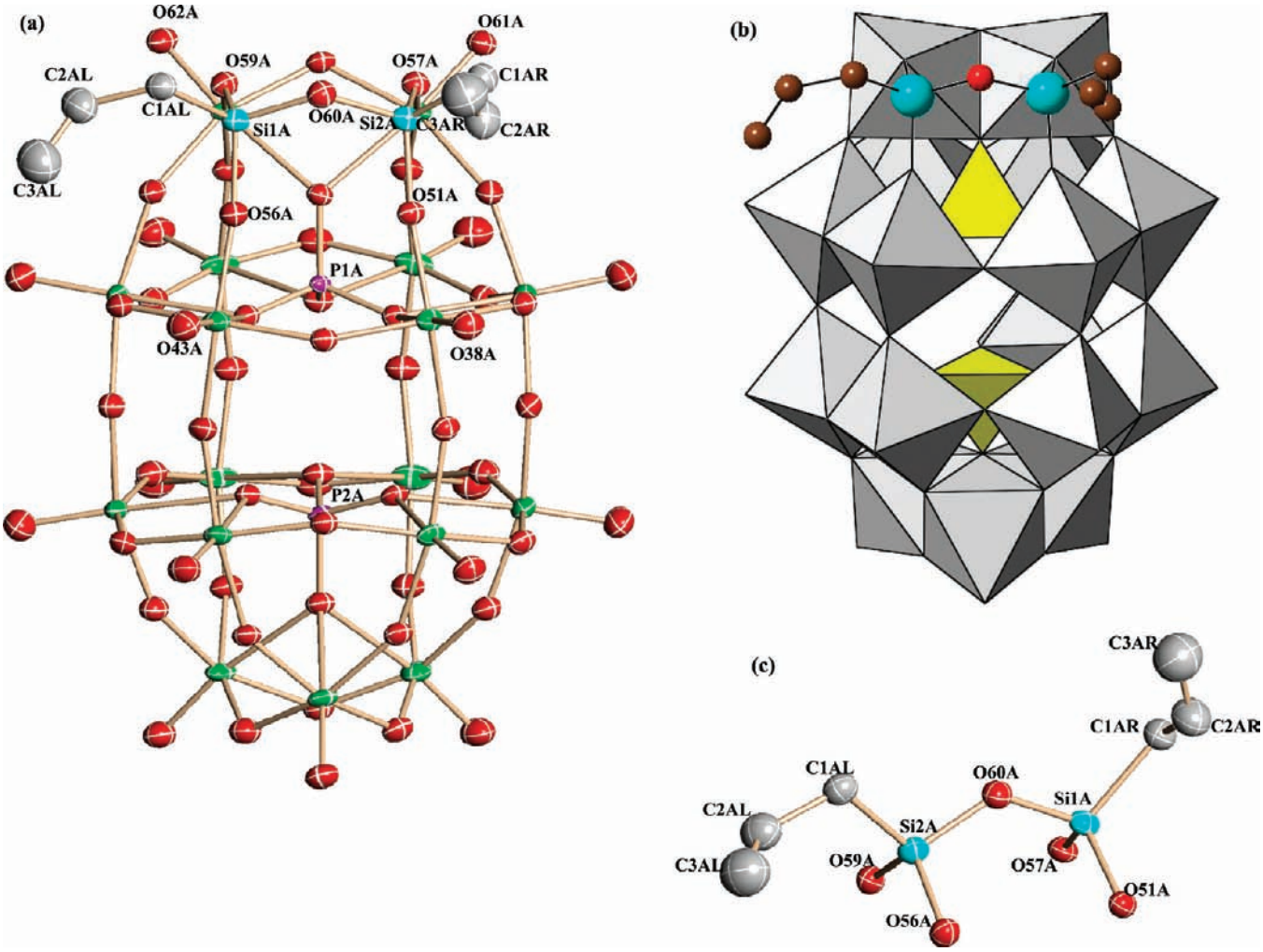

Figure 6. (a) Molecular structure of the polyoxoanion $[\alpha_2\text{-}P_2W_{17}O_{61}\{(H_2C{=}CHCH_2Si)_2O\}]^{6-}$ **Si-2** in **MeN-Si-2** (A-type), (b) its polyhedral representation, and (c) the partial structure around the siloxane bond supported by the polyoxoanion. Designation of color is the same as that in Figure 5.

Thus, the **Ge-1** and **Ge-2** POMs were stable both in solution and in the solid state. In contrast, the **Si-1** and **Si-2** POMs were relatively unstable in H_2O, although they were stable just after dissolving in a 6 M aqueous HCl solution.

CONCLUSION

We have reported the first structure analysis of two organogermyl complexes containing terminal functional groups supported in a monolacunary Dawson POM, $[\alpha_2\text{-}P_2W_{17}O_{61}\{(RGe)\}]^{7-}$ (**Ge-1**, R_1 = $HOOC(CH_2)_2-$ and **Ge-2**, R_2 = $H_2C{=}CHCH_2-$). As related complexes, two novel organosilyl complexes, $[\alpha_2\text{-}P_2W_{17}O_{61}\{(RSi)_2O\}]^{6-}$ (**Si-1**, R_1 and **Si-2**, R_2), were also prepared and unequivocally characterized. In the organogermyl complexes, one organic group was grafted on the inorganic oxide cluster, while in the organosilyl complexes two organic groups were grafted by a siloxane bond. The **Ge-1** and **Ge-2** POMs were stable both in solution and in the solid state. In contrast, the **Si-1** and **Si-2** POMs were relatively unstable in water, although they were stable just after dissolving in a 6 M aqueous HCl solution.

The POMs containing the terminal carboxylic acid group, **Ge-1** and **Si-1**, displayed novel modification of the terminal functional groups. The two POMs containing the allylic groups, **Ge-2** and **Si-2**, could be utilized as precursors for homopolymers and/or copolymers, resulting in the formation of immobilized POM-based catalysts. The present work provides significant information on the molecular architecture of oxide cluster-based inorganic−organic hybrid compounds.

ASSOCIATED CONTENT

Supporting Information. X-ray crystallographic data in CIF format, solid-state ^{31}P CPMAS NMR spectra (Figure S1), ^{31}P NMR in solution (Figure S2), bond lengths and angles for **Ge-1**, **Ge-2**, **Si-1**, and **Si-2** (Tables S1−S4, respectively), and bond valence sum calculations of the W, O, P, and Ge atoms for **Ge-1** and **Ge-2** (Tables S5 and S6) and those of the W, O, P, and Si atoms for **Si-1** and **Si-2** (Tables S7 and S8). This material is available free of charge via the Internet at http://pubs.acs.org.

AUTHOR INFORMATION

Corresponding Author
*E-mail: nomiya@kanagawa-u.ac.jp.

■ ACKNOWLEDGMENT

K.N. acknowledges support by a Grant-in-Aid for Scientific Research (C), No. 22550065, from the Ministry of Education, Culture, Sports, Science and Technology, Japan. We also acknowledge Dr. K. Yoza (Nihon Bruker AXS, Japan) for his assistance on the X-ray structure analysis of **Ge-2** and Dr. T. Hasegawa (R&D Center, KIMOTO CO., Japan) for his advice on synthesis.

■ REFERENCES

(1) (a) Pope, M. T.; Müller, A. *Angew. Chem., Int. Ed. Engl.* **1991**, *30*, 34–48.(b) Pope, M. T. *Heteropoly and Isopoly Oxometalates*; Springer-Verlag: New York, 1983. (c) Day, V. W.; Klemperer, W. G. *Science* **1985**, *228*, 533–541. (d) Hill, C. L. *Chem. Rev.* **1998**, *98*, 1–390. (e) Okuhara, T.; Mizuno, N.; Misono, M. *Adv. Catal.* **1996**, *41*, 113–252. (f) Hill, C. L.; Prosser-McCartha, C. M. *Coord. Chem. Rev.* **1995**, *143*, 407–455. (g) A series of 34 papers in a volume devoted to polyoxoanions in catalysis: Hill, C. L. *J. Mol. Catal. A: Chem.* **1996**, *114*, 1−371. (h) Neumann, R. *Prog. Inorg. Chem.* **1998**, *47*, 317–370. (i) *Polyoxometalate Chemistry from Topology via Self-Assembly to Applications*; Pope, M. T., Müller, A., Eds.; Kluwer Academic Publishers: Dordrecht, The Netherlands, 2001. (j) *Polyoxometalate Chemistry for Nano-Composite Design*; Yamase, T., Pope, M. T., Eds.; Kluwer Academic Publishers: Dordrecht, The Netherlands, 2002. (k) Pope, M. T. In *Comprehensive Coordination Chemistry II*; Wedd, A. G., Ed.; Elsevier Science: New York, 2004; Vol. 4, pp 635−678. (l) Hill, C. L. In *Comprehensive Coordination Chemistry II*; Wedd, A. G., Ed.; Elsevier Science: New York, 2004; Vol. 4, pp 679−759. (m) A series of 32 recent papers in a volume devoted to polyoxometalates in catalysis:Hill, C. L. *J. Mol. Catal. A: Chem.* **2007**, *262*, 1–242. (n) Proust, A.; Thouvenot, R.; Gouzerh, P. *Chem. Commun.* **2008**, 1837–1852. (o) Hasenknopf, B.; Micoine, K.; Lacôte, E.; Thorimbert, S.; Malacria, M.; Thouvenot, R. *Eur. J. Inorg. Chem.* **2008**, 5001–5013. (p) Laurencin, D.; Thouvenot, R.; Boubekeur, K.; Villain, F.; Villanneau, R.; Rohmer, M.-M.; Benard, M.; Proust, A. *Organometallics* **2009**, *28*, 3140–3151. (q) Long, D.-L.; Tsunashima, R.; Cronin, L. *Angew. Chem., Int. Ed.* **2010**, *49*, 1736–1758. (r) Dolbecq, A.; Dumas, E.; Mayer, C. R.; Mialane, P. *Chem. Rev.* **2010**, *110*, 6009–6048. (s) Pradeep, C. P.; Long, D.-L.; Cronin, L. *Dalton Trans.* **2010**, *39*, 9443–9457. (t) Nomiya, K.; Sakai, Y.; Matsunaga, S. *Eur. J. Inorg. Chem.* **2011**, 179–196.

(2) (a) Knoth, W. H. *J. Am. Chem. Soc.* **1979**, *101*, 759–760. (b) Knoth, W. H. *J. Am. Chem. Soc.* **1979**, *101*, 2211–2213. (c) Zonnevijlle, F.; Pope, M. T. *J. Am. Chem. Soc.* **1979**, *101*, 2731–2732. (d) Chorghade, G. S.; Pope, M. T. *J. Am. Chem. Soc.* **1987**, *109*, 5134–5138. (e) Judeinstein, P.; Deprun, C.; Nadjo, L. *J. Chem. Soc., Dalton Trans.* **1991**, 1991–1997. (f) Ammari, N.; Hervé, G.; Thouvenot, R. *New J. Chem.* **1991**, *15*, 607–608. (g) Mayer, C. R.; Thouvenot, R. *J. Chem. Soc., Dalton Trans.* **1998**, 7–14. (h) Mayer, C. R.; Thouvenot, R.; Lalot, T. *Macromolecules* **2000**, *33*, 4433–4437. (i) Mayer, C. R.; Thouvenot, R. *Chem. Mater.* **2000**, *12*, 257–260. (j) Sanchez, C.; Soler-Illia, G.; Ribot, F.; Lalot, T.; Mayer, C. R.; Cabuil, V. *Chem. Mater.* **2001**, *13*, 3061–3083. (k) Mayer, C. R.; Neveu, S.; Cabuil, V. *Angew. Chem., Int. Ed.* **2002**, *41*, 501–503. (l) Mayer, C. R.; Hervé, M.; Lavanant, H.; Blais, J.-C.; Sécheresse, F. *Eur. J. Inorg. Chem.* **2004**, 973–977. (m) Mayer, C. R.; Roch-Marchal, C.; Lavanant, H.; Thouvenot, R.; Sellier, N.; Blais, J.-C.; Sécheresse, F. *Chem.—Eur. J.* **2004**, *10*, 5517–5523. (n) Bareyt, S.; Piligkos, S.; Hasenknopf, B.; Gouzerh, P.; Lacôte, E.; Thorimbert, S.; Malacria, M. *J. Am. Chem. Soc.* **2005**, *127*, 6788–6794. (o) Cannizzo, C.; Mayer, C. R.; Sécheresse, F.; Larpent, C. *Adv. Mater.* **2005**, *17*, 2888–2892. (p) Hasegawa, T.; Murakami, H.; Shimizu, K.; Kasahara, Y.; Yoshida, S.; Kurashina, T.; Seki, H.; Nomiya, K. *Inorg. Chim. Acta* **2008**, *361*, 1385–1394. (q) Duffort, V.; Thouvenot, R.; Afonso, C.; Izzet, G.; Proust, A. *Chem. Commun.* **2009**, 6062–6064.

(3) (a) Kim, G. S.; Hagen, K. S.; Hill, C. L. *Inorg. Chem.* **1992**, *31*, 5316–5324. (b) Wei, X.; Dickman, M. H.; Pope, M. T. *Inorg. Chem.* **1997**, *36*, 130–131. (c) Wei, X.; Dickman, M. H.; Pope, M. T. *J. Am. Chem. Soc.* **1998**, *120*, 10254–10255. (d) Radkov, E. V.; Beer, R. H. *Inorg. Chim. Acta* **2000**, *297*, 191–198. (e) Sveshnikov, N. N.; Dickman, M. H.; Pope, M. T. *Inorg. Chim. Acta* **2006**, *359*, 2721–2727. (f) Sun, Z.-G.; Zhang, L.-C.; Liu, Z.-M.; Cui, L.-Y.; Tian, C.-H.; Liang, H.-D.; Zhu, Z.-M.; You, W.-S. *J. Coord. Chem.* **2006**, *59*, 1557–1564. (g) Liu, H.; Gómez-García, C. J.; Peng, J.; Sha, J.; Wang, L.; Yan, Y. *Inorg. Chim. Acta* **2009**, *362*, 1957–1962.

(4) (a) Xin, F.; Pope, M. T. *Inorg. Chem.* **1996**, *35*, 5693–5695. (b) Mayer, C. R.; Herson, P.; Thouvenot, R. *Inorg. Chem.* **1999**, *38*, 6152–6158. (c) Mazeaud, A.; Dromzee, Y.; Thouvenot, R. *Inorg. Chem.* **2000**, *39*, 4735–4740.

(5) (a) Xin, F.; Pope, M. T. *Organometallics* **1994**, *13*, 4881–4886. (b) Xin, F.; Pope, M. T.; Long, G. J.; Russo, U. *Inorg. Chem.* **1996**, *35*, 1207–1213. (c) Maseaud, A.; Ammari, N.; Robert, F.; Thouvenot, R. *Angew. Chem., Int. Ed. Engl.* **1996**, *35*, 1961–1964. (d) Sazani, G.; Dickman, M. H.; Pope, M. T. *Inorg. Chem.* **2000**, *39*, 939–943. (e) Niu, J.; Li, M.; Wang, J. *J. Organomet. Chem.* **2003**, *675*, 84–90. (f) Niu, J.; Zhao, J.; Wang, J.; Li, M. *J. Mol. Struct.* **2003**, *655*, 243–250. (g) Agustin, D.; Coelho, C.; Mazeaud, A.; Herson, P.; Proust, A.; Thouvenot, R. *Anorg. Allg. Chem.* **2004**, *630*, 2049–2053. (h) Hussain, F.; Kortz, U. *Chem. Commun.* **2005**, 1191–1193. (i) Kortz, U.; Hussain, F.; Reicke, M. *Angew. Chem., Int. Ed.* **2005**, *44*, 3773–3777. (j) Belai, N.; Pope, M. T. *Polyhedron* **2006**, *25*, 2015–2020. (k) Hussain, F.; Dickman, M. H.; Kortz, U.; Keita, B.; Nadjo, L.; Khitrov, G. A.; Marshall, A. G. *J. Cluster. Sci.* **2007**, *18*, 173–191. (l) Khoshnavazi, R.; Bahrami, L. *J. Coord. Chem.* **2009**, *62*, 2067–2075. (m) Piedra-Garza, L. F.; Dickman, M. H.; Moldovan, O.; Breunig, H. J.; Kortz, U. *Inorg. Chem.* **2009**, *48*, 411–413. (n) Reinoso, S.; Piedra-Garza, L. F.; Dickman, M. H.; Praetorius, A.; Biesemans, M.; Willem, R.; Kortz, U. *Dalton Trans.* **2010**, 248–255. (o) Reinoso, S.; Bassil, B. S.; Barsukova, M.; Kortz, U. *Eur. J. Inorg. Chem.* **2010**, 2537–2542. (p) Aoki, S.; Kurashina, T.; Kasahara, Y.; Nishijima, T.; Nomiya, K. *Dalton Trans.* **2011**, *40*, 1243–1253.

(6) (a) Sakai, Y.; Shinohara, A.; Hayashi, K.; Nomiya, K. *Eur. J. Inorg. Chem.* **2006**, 163–171. (b) Kato, C. N.; Kasahara, Y.; Hayashi, K.; Yamaguchi, A.; Hasegawa, T.; Nomiya, K. *Eur. J. Inorg. Chem.* **2006**, 4834–4842. (c) Hasegawa, T.; Kasahara, Y.; Yoshida, S.; Kurashina, T.; Aoki, S.; Yoza, K.; Nomiya, K. *Inorg. Chem. Commun.* **2007**, *10*, 1416–1419. (d) Hasegawa, T.; Shimizu, K.; Seki, H.; Murakami, H.; Yoshida, S.; Yoza, K.; Nomiya, K. *Inorg. Chem. Commun.* **2007**, *10*, 1140–1144. (e) Kurashina, T.; Aoki, S.; Hirasawa, R.; Hasegawa, T.; Kasahara, Y.; Yoshida, S.; Yoza, K.; Nomiya, K. *Dalton Trans.* **2009**, 5542–5550. (f) Pradeep, C. P.; Misdrahi, M. F.; Li, F.-Y.; Zhang, J.; Xu, L.; Long, D.-L.; Liu, T.; Cronin, L. *Angew. Chem., Int. Ed.* **2009**, *48*, 8309–8313. (g) Zhang, L. C.; Zheng, S. L.; Xue, H.; Zhu, Z. M.; You, W. S.; Li, Y. G.; Wang, E. *Dalton Trans.* **2010**, 3369–3371.

(7) (a) Hussain, F.; Kortz, U.; Clark, R. J. *Inorg. Chem.* **2004**, *43*, 3237–3241. (b) Reinoso, S.; Dickman, M. H.; Matei, M. F.; Kortz, U. *Inorg. Chem.* **2007**, *46*, 4383–4385. (c) Reinoso, S.; Dickman, M. H.; Praetorius, A.; Piedra-Garza, L. F.; Kortz, U. *Inorg. Chem.* **2008**, *47*, 8798–8806. (d) Reinoso, S.; Dickman, M. H.; Kortz, U. *Eur. J. Inorg. Chem.* **2009**, 947–953. (e) Zhang, L. C.; Xue, H.; Zhu, Z. M.; Wang, Q. X.; You, W. S.; Li, Y. G.; Wang, E. B. *Inorg. Chem. Commun.* **2010**, *13*, 609–612.

(8) (a) Sazani, G.; Pope, M. T. *Dalton Trans.* **2004**, 1989–1994. (b) Joo, N.; Renaudineau, S.; Delapierre, G.; Bidan, G.; Chamoreau, L.-M.; Thouvenot, R.; Gouzerh, P.; Proust, A. *Chem.—Eur. J.* **2010**, *16*, 5043–5051. (c) Li, J.; Tan, R.; Li, R.; Wang, X.; Li, E.; Zhai, F.; Zhang, S. *Inorg. Chem. Commun.* **2007**, *10*, 216–219. (d) Li, J.; Zhai, F.; Wang, X.; Li, E.; Zhang, S.; Zhang, Q.; Du, X. *Polyhedron* **2008**, *27*, 1150–1154.

(9) (a) Horan, J. L.; Genupur, A.; Ren, H.; Sikora, B. J.; Kuo, M.-C.; Meng, F.; Dec, S. F.; Haugen, G. M.; Yandrasits, M. A.; Hamrock, S. J.; Frey, M. H.; Herring, A. M. *ChemSusChem* **2009**, *2*, 226–229. (b) Okura, H.; Okumura, Y.; Shibata, M.; Kumagai, M.; Nomiya, K. U.S. Patent 2008268326, 2008.

(10) Rocchiccioli-Deltcheff, C.; Thouvenot, R. *Spectrosc. Lett.* **1979**, *12*, 127–138.

(11) (a) Brown, I. D.; Altermatt, D. *Acta Crystallogr., Sect. B* **1985**, *B41*, 244–247. (b) Brown, I. D.; Shannon, R. D. *Acta Crystallogr., Sect. A* **1973**, *A29*, 266–282. (c) Brown, I. D. *Acta Crystallogr., Sect. B* **1992**,

B48, 553–572. (d) Brown, I. D. *J. Appl. Crystallogr.* **1996**, *29*, 479–480.

(12) (a) Lyon, D. K.; Miller, W. K.; Novet, T.; Domaille, P. J.; Evitt, E.; Johnson, D. C.; Finke, R. G. *J. Am. Chem. Soc.* **1991**, *113*, 7209–7221. (b) Contant, R. *Inorg. Synth.* **1990**, *27*, 104–111.

(13) (a) Sheldrick, G. M. *Acta Crystallogr., Sect. A* **1990**, *46*, 467–473. (b) Sheldrick, G. M. *SHELXL-97 Program for Crystal Structure Refinement*; University of Göttingen: Göttingen, Germany, 1997. (c) Sheldrick, G. M. *SADABS*; University of Göttingen: Göttingen, Germany, 1996.